NAVAL POSTGRADUATE SCHOOL

MONTEREY, CALIFORNIA

THESIS

GAS TURBINE OPERATION ON COMPRESSED HYDROGEN

by

Jennifer N. Penley

December 2018

Thesis Advisor:	Garth V. Hobson
Co-Advisor:	Anthony J. Gannon
Second Reader:	Andrea D. Holmes

THIS PAGE INTENTIONALLY LEFT BLANK

REPORT DOCUMENTATION PAGE			*Form Approved OMB No. 0704-0188*

1. AGENCY USE ONLY *(Leave blank)*	**2. REPORT DATE** December 2018	**3. REPORT TYPE AND DATES COVERED** Master's thesis

4. TITLE AND SUBTITLE GAS TURBINE OPERATION ON COMPRESSED HYDROGEN	**5. FUNDING NUMBERS**
6. AUTHOR(S) Jennifer N. Penley	
7. PERFORMING ORGANIZATION NAME(S) AND ADDRESS(ES) Naval Postgraduate School Monterey, CA 93943-5000	**8. PERFORMING ORGANIZATION REPORT NUMBER**
9. SPONSORING / MONITORING AGENCY NAME(S) AND ADDRESS(ES) N/A	**10. SPONSORING / MONITORING AGENCY REPORT NUMBER**

11. SUPPLEMENTARY NOTES The views expressed in this thesis are those of the author and do not reflect the official policy or position of the Department of Defense or the U.S. Government.

12a. DISTRIBUTION / AVAILABILITY STATEMENT Approved for public release. Distribution is unlimited.	**12b. DISTRIBUTION CODE** A

13. ABSTRACT (maximum 200 words)

The purpose of this thesis was to effectively run a small turbojet engine using compressed hydrogen gas and then baseline a microturbine using propane. These baselines provide the data collection needed in order to develop an overall plan for running a microturbine using compressed hydrogen gas. The turbojet engine was designed to simulate a full-size turbojet engine and run it off liquid fuel. To baseline this turbojet engine and understand its normal operating parameters, it was successfully operated using kerosene gas. The results of the liquid fuel operation were compared to the successful operation of the same turbojet engine using hydrogen. The Capstone C30 microturbine was selected for its power generation and small, practical size. This microturbine was baselined using propane, for which it was originally designed, and it displayed the expected results. The steps taken in this thesis help lead toward the ultimate goal of developing a system where a microturbine runs off the stored hydrogen to create a small, portable, and inexpensive system that produces a high amount of energy with no toxic emissions.

14. SUBJECT TERMS energy, hydrogen, turbine	**15. NUMBER OF PAGES** 91
	16. PRICE CODE

17. SECURITY CLASSIFICATION OF REPORT	**18. SECURITY CLASSIFICATION OF THIS PAGE**	**19. SECURITY CLASSIFICATION OF ABSTRACT**	**20. LIMITATION OF ABSTRACT**
Unclassified	Unclassified	Unclassified	UU

NSN 7540-01-280-5500 Standard Form 298 (Rev. 2-89) Prescribed by ANSI Std. 239-18

THIS PAGE INTENTIONALLY LEFT BLANK

Approved for public release. Distribution is unlimited.

GAS TURBINE OPERATION ON COMPRESSED HYDROGEN

Jennifer N. Penley
Lieutenant, United States Navy
BS, U.S. Naval Academy, 2013

Submitted in partial fulfillment of the
requirements for the degree of

MASTER OF SCIENCE IN MECHANICAL ENGINEERING

from the

NAVAL POSTGRADUATE SCHOOL
December 2018

Approved by: Garth V. Hobson
Advisor

Anthony J. Gannon
Co-Advisor

Andrea D. Holmes
Second Reader

Garth V. Hobson
Chair, Department of Mechanical and Aerospace Engineering

THIS PAGE INTENTIONALLY LEFT BLANK

ABSTRACT

The purpose of this thesis was to effectively run a small turbojet engine using compressed hydrogen gas and then baseline a microturbine using propane. These baselines provide the data collection needed in order to develop an overall plan for running a microturbine using compressed hydrogen gas. The turbojet engine was designed to simulate a full-size turbojet engine and run it off liquid fuel. To baseline this turbojet engine and understand its normal operating parameters, it was successfully operated using kerosene gas. The results of the liquid fuel operation were compared to the successful operation of the same turbojet engine using hydrogen. The Capstone C30 microturbine was selected for its power generation and small, practical size. This microturbine was baselined using propane, for which it was originally designed, and it displayed the expected results. The steps taken in this thesis help lead toward the ultimate goal of developing a system where a microturbine runs off the stored hydrogen to create a small, portable, and inexpensive system that produces a high amount of energy with no toxic emissions.

THIS PAGE INTENTIONALLY LEFT BLANK

TABLE OF CONTENTS

LIST OF FIGURES

LIST OF TABLES

THIS PAGE INTENTIONALLY LEFT BLANK

LIST OF ACRONYMS AND ABBREVIATIONS

BTU	British Thermal Unit
DoD	Department of Defense
DoN	Department of the Navy
FY	Fiscal Year
GW	Gigawatt
kW	kilowatt
kWh	kilowatt-hour
lb	pound
LHV	Lower Heating Value
MPa	Megapascal
psi	pound per square inch
rpm	revolutions per minute
Pa	Pascal
deg C	degrees Celsius
deg F	degrees Fahrenheit
in	inch
psig	pounds per square inch (gauge)
s	seconds
deg R	degree Rankine
deg K	degree Kelvin
kg	kilogram

THIS PAGE INTENTIONALLY LEFT BLANK

ACKNOWLEDGMENTS

I would like to thank my family for their continued support and love throughout my study and education at the Naval Postgraduate School. I would also like to thank Dr. Garth Hobson and Dr. Anthony Gannon for their dedication and leadership through the project, as well as Ms. Andrea Holmes and Mr. John Gibson for their support and guidance throughout the project. Lastly, many thanks to the Rocket Propulsion Lab staff, Mr. Robert Wright, Mr. David Dausen, and Dr. Christopher Brophy, who provided expertise, material, and advice to help the project's success.

THIS PAGE INTENTIONALLY LEFT BLANK

I. INTRODUCTION

The purpose of this research is to continue the development of a renewable hydrogen plant that will provide the fuel for a hydrogen powered gas turbine. The research is intended to further the ongoing efforts to develop low-cost hydrogen infrastructure in the Navy, funded by the Office of Naval Research Engineering Systems Technology Evaluation Program. This research has the potential to generate renewable power with expeditionary microgrids and sea-based hydrogen harvesting.

A. MOTIVATION

Similar to industry, the Department of Defense (DoD), specifically the Department of the Navy (DoN), relies heavily on electricity and carbon-based fuels. However, both entities are making strides to reduce energy consumption and further renewable energy exploration. In 2009, the Secretary of the Navy promulgated energy goals, to include that "by 2020, DoN will produce 50% of its energy from alternative sources. In support of this alternative energy goal, Secretary Mabus chartered the 1 Gigawatt Task Force (1GW TF) to enable DoN to procure one gigawatt (GW) of renewable energy generation capacity by 2020" [1]. To accomplish these goals, the DoN has considered all potential sources of renewable energy applications.

Currently, the DoN installations rely heavily on local power companies to supply and support energy needs. This can be costly but is often the most reliable and resilient source of energy supply. The DoN has been working to diversify its means of energy supply sources on its installations through renewable or distributed energy. In FY 2015, the DoD had approximately 1,390 active renewable energy projects and within one year, increased it by approximately 17% to reach 1,631 active projects [2]. The most significant source of renewable energy in DoD installations is geothermal electric power and is the most abundant energy supply of the approximately 12,900 billion Btus of renewable energy that were produced or procured in FY 2016 [2]. Other forms of renewable energy that contribute to the DoD energy supply are shown in Figure 1.

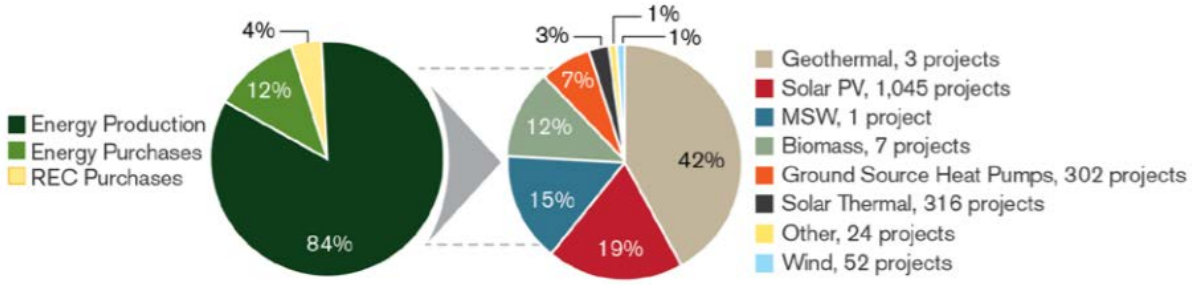

Figure 1. DoD renewable energy supply mix by technology type in FY 2016. Source: [2].

The need for renewable energy generation is growing, especially within the DoN due to the large amounts of energy that each platform uses daily. Currently, the DoN has been expanding its resources to explore new forms of renewable energy in order to reach its goals set by the Secretary of the Navy of producing 1GW of renewable energy, "sourcing at least 50% of shore-based energy from alternative sources, and having 50% of installations achieve net-zero by 2020" [1]. Wind and solar explorations are expensive, and energy production is often intermittent and hard to predict. Although this technology is mature, it is often challenging due to inefficiencies, space constraints, and energy storage constraints. Geothermal and biogenic energies have proven to be good sources of energy that are capable of full-time baseload power, but exploration can be difficult and expensive [1]. Therefore, as renewable energy generation needs increase, the DoN needs to continually develop and explore new efficient and cost-effective ways to generate, store, and use renewable energy. Hydrogen is the most occurring component taking up 75% of the universe and combined with oxygen forms water. Because hydrogen is such an abundant resource, it is essentially infinite and is a clean and non-toxic energy source [3]. Hydrogen, with a higher heating value more than twice that of petroleum fuels, has the potential to be properly harnessed in an efficient and cost-effective way, making the possibilities for renewable energy infinite.

Hickam Air Force Base uses a hydrogen system, HydraFLX, that generates ultra-pure hydrogen from sea water in a flexible pressure management process to fuel vehicles

and other support equipment using fuel cells to convert the hydrogen gas to consumable energy [4]. Although fuel cells are a convenient way to convert hydrogen to energy, this research aims to use hydrogen to power a gas turbine engine. Fuel cells and microturbines have many of the same advantages as far as high efficiencies and low emissions. Microturbines also are known for their low maintenance requirements, flexible design capability, and reliability [5]. Using hydrogen to safely power a gas turbine engine has the potential to change the way hydrogen energy is harnessed and create a new and functional clean energy source.

B. LITERATURE REVIEW

Hydrogen renewable energy has become increasingly popular due to its abundance clean output, and high energy potential. However, harnessing hydrogen for proper and safe use creates challenges that must be considered when producing, storing, and using it for fuel. "Current production of hydrogen is about 55 million U.S. tons/year, mostly for industrial purposes in chemical and petro-chemical applications. A world economy using hydrogen as a major energy carrier will require a tremendous increase in that volume, as well as a complex new infrastructure for transporting and delivering hydrogen to end users" [6]. The infrastructure would require technological advancements to overcome significant hurdles to make hydrogen systems safe and practical.

As the world energy consumption continues to increase rapidly, the need for fuel sources that release less CO_2 per unit of energy also increases [6]. Many nations are moving toward the funding and implementation of cleaner energy that is more environmentally friendly and practical. Currently, the main sources of renewable energy are wind and geothermal; however, they can provide only a limited portion of the energy needed [6]. Hydrogen contains no carbon, meaning that when it is burned, it generates only water, heat, and energy. Except for traces created from the lubricant, and in the absence of other carbon compounds, nitrogen oxides are the only pollutants that result from hydrogen-fueled engines. During a combustion process, nitric oxide, which is one of the main ozone depleting gases, is the main species emitted into the atmosphere [7].

The most economic means at this time for producing hydrogen is through carbon capture and storage (CCS), steam reforming which produces hydrogen through natural gas, or processes that use coal reserves such as gasification, partial oxidation, or autothermal reforming [6]. The potential for hydrogen to be created through other renewable resources is practical and would create energy with no carbon emission.

Production of hydrogen that completely removes CO_2 from the process is the first obstacle. Electrolysis produces hydrogen from water and electricity but 10%–30% of the input energy is lost; nonetheless, this could be a sensible means of generating hydrogen if the cost of the primary electricity is minimal [6]. It is unclear at the moment whether producing hydrogen through conversion of non-polluting electricity sources such as solar, wind, nuclear, or biomass is a viable option for society as a whole because of the significant losses associated with each process. The issues associated with efficient hydrogen production are slowly being tackled, but in some cases, the technology could be decades away.

An additional hurdle in making hydrogen a feasible option for society is the transportation and distribution. Almost 96% of hydrogen production is consumed locally, with the market for merchant hydrogen in the United States being the most established, with just over 15% being transported for off-site use [6]. Cost is a significant challenge when discussing hydrogen transportation and distribution and can be broken down into two parts: pipeline systems and dispensing. Hydrogen pipelines with larger diameters, some estimates close to 30 inches, may be required to provide widespread hydrogen infrastructure but are expected to cost much more due to the materials needed to resist hydrogen embrittlement and labor of hydrogen-specific welding [6]. Furthermore, dispensing the hydrogen for personal use requires a safe and reasonable means for dispensing to be developed. “It is estimated that about 180,000 filling stations will need to be converted to hydrogen in the USA and about 135,000 stations in Europe” [6]. Converting the filling stations could require extensive piping systems or local production, but the technology to do so in safe, fast, and convenient ways has yet to be discovered.

Although transporting and dispersion have their challenges, the capability for localized storage is considered the ultimate obstacle to achieve in mobilizing the use of

hydrogen [6]. Hydrogen is storable as a liquid, compressed gas, or as a metal, also known as a chemical hydride. Compared to gasoline, liquid hydrogen has the highest energy density but is approximately one-third of the volumetric value [6]. For safety concerns, hydrogen gas must be bled off to lower the risk of pressure build-up, making liquid hydrogen storage not a sustainable possibility for portable long-term storage [6]. Chemical hydrides are being researched for hydrogen storage because although the process to get hydrogen into the hydride is safe and stable, it is time consuming and requires high temperatures [6].

Safety is the underlying theme for each challenge regarding the future of hydrogen use. Hydrogen testing is being done to understand the effects of hydrogen use in regard to climate and air pollution but also to develop hydrogen safety sensors that alert users in hazardous situations [6]. Hydrogen has different flammability characteristics and concentration limits from other gasses such as propane or methane that have been used as fuel in the past. Currently, hydrogen is mainly used in industry use where handlers are trained on the proper handling. Transitioning to a hydrogen gas for the general population would require training and time for acceptance and time to become familiar with the new fuel source. Further development of safety procedures and easy to understand literature on hydrogen use would have to be put in place and widely understood before hydrogen can be implemented.

The advances necessary to support an achievable hydrogen economy are substantial and will require endurance for scientists, engineers, and the countries with plans for implementation. The benefits of harnessing hydrogen as a clean energy are also associated with challenges such as cost, durability, efficiency improvements, and material embrittlement [6]. The hydrogen obstacles can be broken down into four basic parts: production, transport and distribution, storage, and safety.

A system using hydrogen as a major carrier throughout the energy cycle is known as a hydrogen economy [6]. Many influencing countries have plans to develop a hydrogen-oriented economy but span several decades and include complete development of new infrastructure, hydrogen production, delivery, and storage methods, and continuous public education and outreach as the use of hydrogen can potentially disrupt society [6]. A recent

study predicts that by 2020, Europe will have over 6 million active hydrogen-powered cars which is similar to Japan's goal to have 5 million active fuel cell vehicles with a fixed fuel cell generation system with a 10 GW capacity by 2020 [6]. European Union's (EU) roadmap for executing a potential hydrogen economy and fuel cell development is shown in Figure 2.

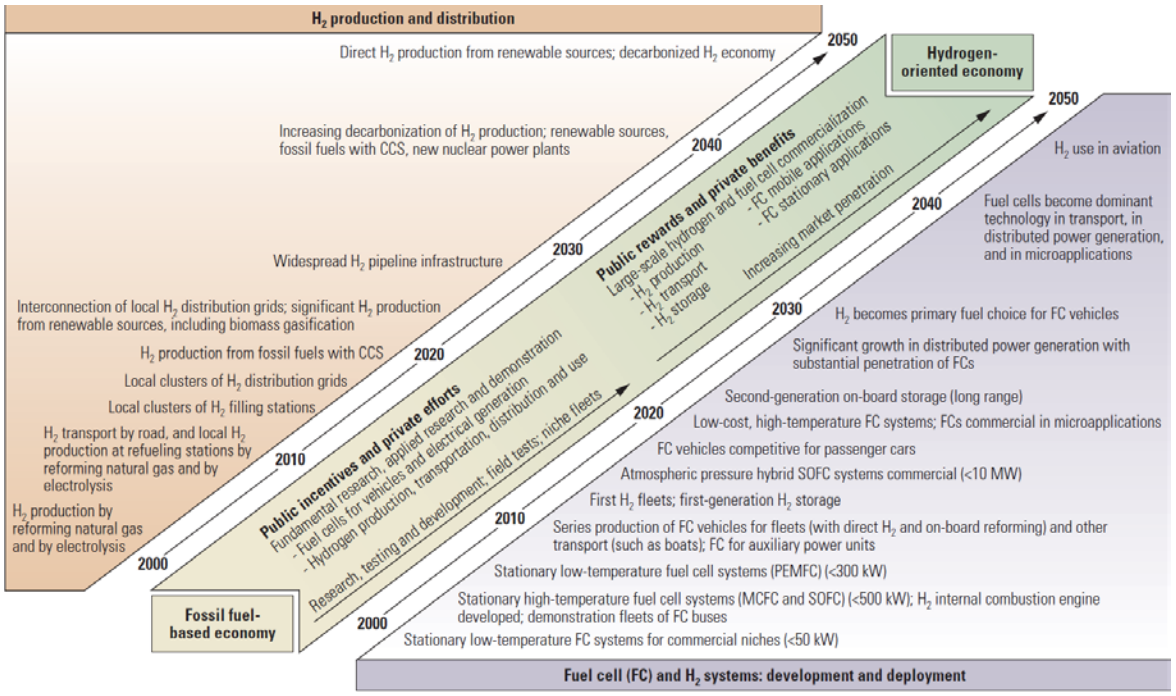

Figure 2. European Union estimated timeline for implementing a hydrogen economy. Source: [6].

Currently, the United States and the and EU have large active projects to research and develop energy using hydrogen. FurtureGen in the U.S. and HYPOGEN in the EU are both developing power plants that convert energy from coal and fossil fuels, respectively, that result in zero undesirable emissions [6]. The EU's program, HYCOM, was created to demonstrate an entire community using hydrogen infrastructure, while the U.S. Hydrogen Fuels Initiative plans make fuel cell vehicles a practical and economical option for the general public by 2020 [6]. ENEL, a European company, introduced the world's first industrial scale hydrogen-fueled combined cycle plant in 2010 based in Venice, Italy, that

generates clean electricity to meet the annual needs of 20,000 households and eliminates adding more than 17,000 metric tons of CO_2 emissions a year [8]. The U.S. Department of Energy has a number of projects that incorporate hydrogen use and research the possibility of hydrogen production through different means. The Lawrence Berkeley National Laboratory has conducted research using low-emission gas turbines that are fueled by pure hydrogen and use low-swirl injector technology that is predicted to eliminate tons of carbon dioxide and nitrous oxides from power plants every year [9]. As previously mentioned, Hickam Air Force Base in Hawaii introduced a solar-panel powered local hydrogen generation system and dispensing station that helps power fuel-cell powered vehicles and cut down on energy costs for the Air Force and Hawaii's oil dependence [4]. With all of these different companies and programs, pursuit of renewable clean energy is a priority worldwide with a clear focus on the potential of hydrogen energy. The timeline for implementation is extensive but also requires multiple advancements and coordination between many entities.

Developing hydrogen-fueled energy is an important step on the path to clean energy. Its benefits are substantial but that pairs with significant challenges that need to be overcome to create and implement safe and viable options for public use. Worldwide companies such as Schlumberger, ExxonMobil, GE, and Toyota have committed to a Global Climate and Energy Project with efforts to build a diverse profile of technology projects that reduce greenhouse-gas emissions [6]. "The future energy supply is likely to be a mixture of many sources, including fossil fuels, nuclear and green energy, with hydrogen and electricity as carrier" [6]. As innovations continue to move toward the next phase of advanced energy supply, energy leaders will have to continue to evaluate economics and how energy markets are driven by cost-benefit analyses. The government push in the U.S. and Europe is important for the hydrogen economy development but does not mean that a feasible hydrogen economy will develop in the near future. With the challenges that a hydrogen-based economy offers, cost and safety must be considered in all scenarios while developing the hydrogen economy.

C. PREVIOUS WORK

This project was created with the objective to evaluate and test new alternative energy technologies for the Navy and Marine Corps. Due to high dependency on fossil fuels, it is important that the DoD become more energy efficient and move toward the Secretary of the Navy's goal that the DoN will produce 50% of its energy using alternative sources [1].

1. HYDROGEN GENERATION

a. Hydrogen Creation

The project was initially developed to design and prototype a system that would reduce dependency on fossil fuels by proving the concept of a solar powered hydrogen production facility [10]. In 2016, Aviles' thesis on renewable hydrogen energy used commercial-off-the-shelf components to accomplish the initial objective for the design and to be considered a new alternative technology [10]. The system generated hydrogen to power a fuel cell that provided data on the feasibility of the research goal. It used four dehumidifiers to produce distilled water that was then stored in internal tanks within the unit and required manual operation of the alkaline electrolyzer in order to supply a proper amount of potassium hydroxide. The data was then used with a scalability factor to determine if a large-scale system could be cost effective in the future [10]. However, this initial system required extensive operator interaction and little regulation of the power needs of the system.

In 2017, Yu successfully completed thesis research to improve the solar-powered hydrogen generation system for sustained hydrogen production [11]. Yu understood that when the electrolyzer fed hydrogen and oxygen to the respective process tanks and water is disassociated, it produced a larger gaseous volume of hydrogen than oxygen, which created a pressure differential between the two process tanks. This differential was addressed by the operator manually adjusting a needle valve that allowed more oxygen gas to escape so the volume of each gas leaving the system would be the same [11]. Through many different tools and efficiencies, the system was able to regulate the hydrogen energy production proving that hydrogen production using renewable energy was effective and

could generate electric power using a small fuel cell. The overall hydrogen generation system is shown in Figure 3.

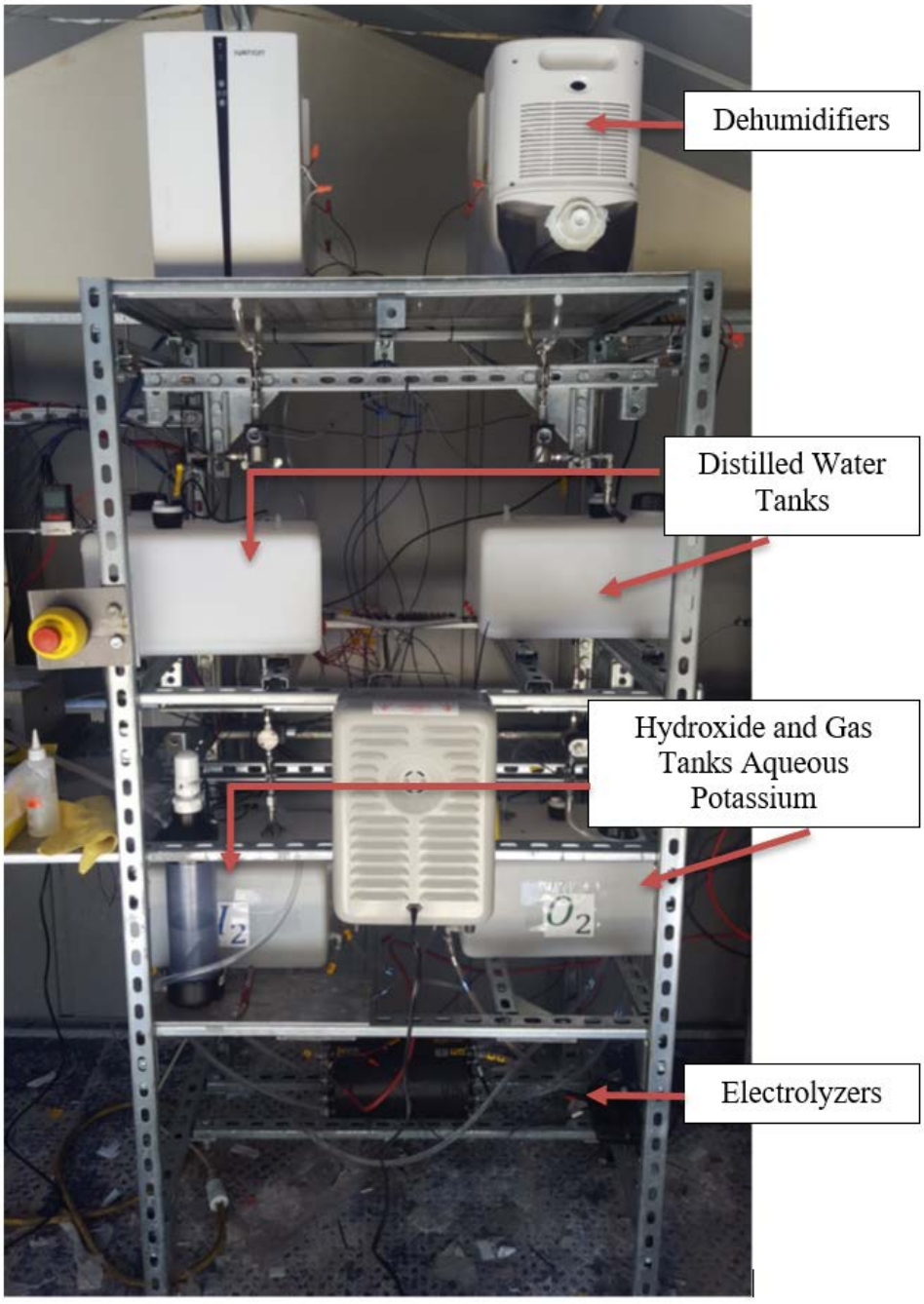

Figure 3. Overall solar-powered system design for hydrogen generation

b. Hydrogen Production Automation

The next step in hydrogen generation was to automate the process, as the goal of the system is to be a feasible, commercialize system [12]. Birkemeier created two programs to ensure safe operation of the system described previously, and shown in Figure 3: a normal operation program and an emergency shutdown program [12]. The normal operation program controls startup, shutdown, and normal system operation while the emergency shutdown program is only used if an emergency condition is detected by the operator or an installed safety device. The logic flow diagram for the program is shown in Figure 4. Birkemeier designed the system for the normal operation program to be the backbone for the system to produce hydrogen successfully and safely. The automated production testing proved that the current system could be scaled up to meet hydrogen requirements as necessary given proper sensors and dehumidifiers [12].

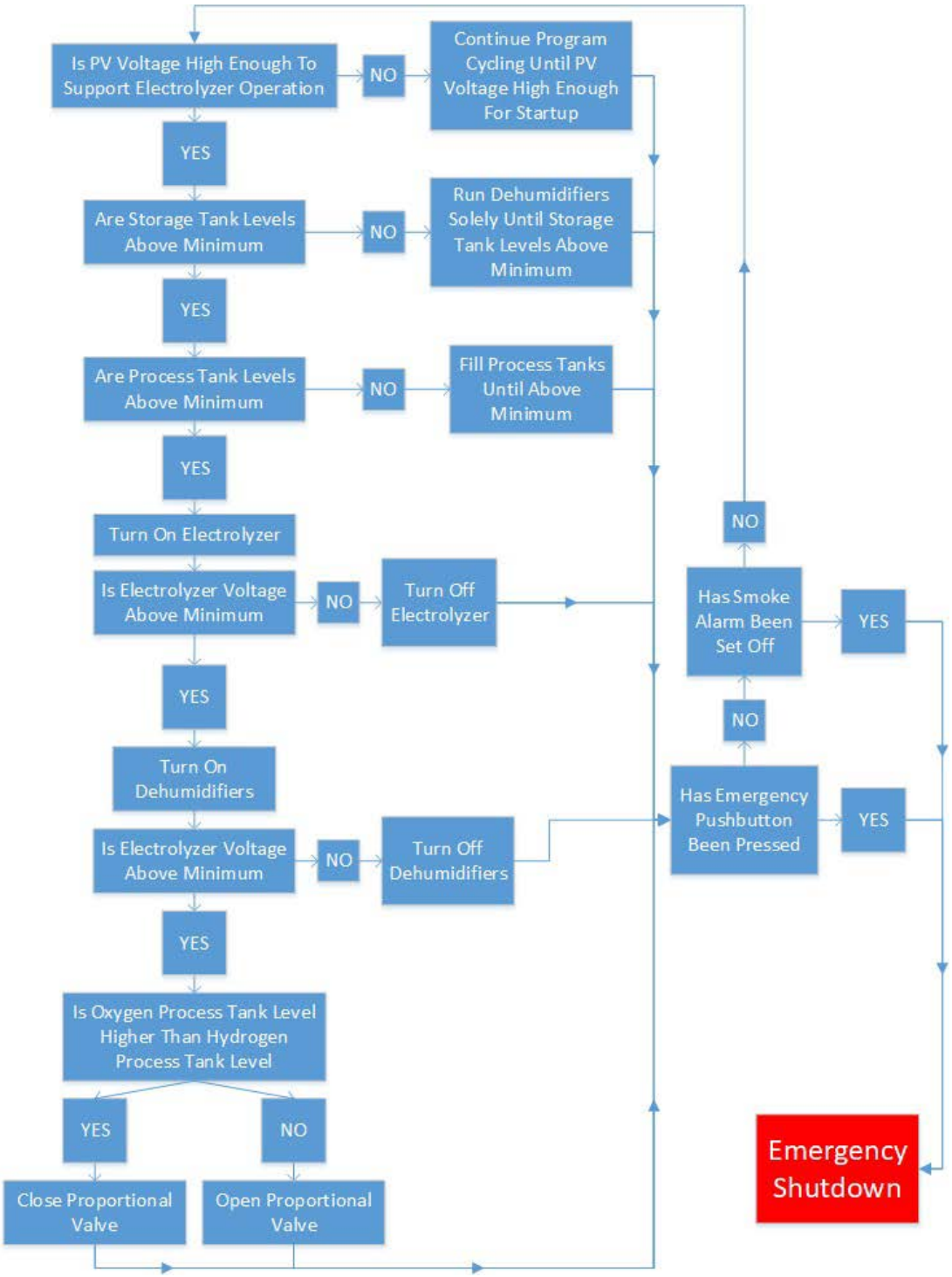

Figure 4. Logic flow for hydrogen generation automation system. Source: [12].

The controller shown in Figure 5 was an Allen Bradley Micro850 controller with plug in and expansion modules that was used to implement the logic shown in Figure 4. The code and details of implementation are found in Birkemeier's thesis [12].

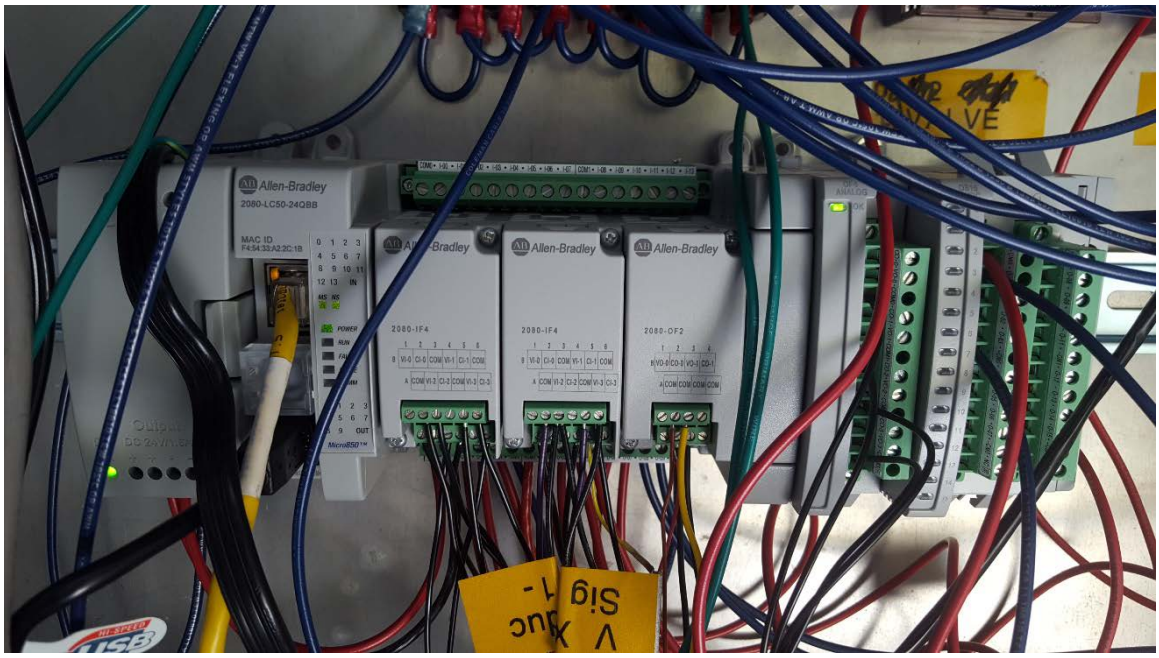

Figure 5. Allen Bradley Micro850 controller used to implement hydrogen production automation. Source: [12] .

2. HYDROGEN STORAGE

After the hydrogen is generated, the next task for this project was to safely store and compress the hydrogen gas. The details regarding the intricacies of the compressed hydrogen system are described in Fossen's thesis [13]; however, Fossen established the foundation for the hydrogen compression system as an electrochemical compressor [13]. This compressor uses direct current to transport hydrogen molecules through a proton exchange membrane to increase pressure and are known to have higher efficiencies and longer operational cycles than traditional compressors [13].

Storage of the hydrogen gas also necessitated a system that required multiple safety devices [13]. Mainly, rupture disks and relief valves which vent to the atmosphere were located throughout the system to protect from over compression of the hydrogen gas [13].

Designing a flexible and successful compressed hydrogen storage system allowed for continued growth of the system and for the system to be easily connected to any power source for compressed hydrogen gas use. The hydrogen storage containers are shown in Figure 6.

Figure 6. All-steel, standard size, compressed gas cylinders used for hydrogen storage

THIS PAGE INTENTIONALLY LEFT BLANK

II. ENABLING TECHNOLOGY

A. TURBINE ENGINE

1. Sophia J450 Turbojet Engine

The Sophia J450 turbojet engine was designed to model an actual full-size turbojet engine for research and testing purposes. As this turbojet engine was designed to act very similar to an actual full-size turbojet engine, the components operate in the same manner [14]. The air enters the air intake, is compressed by the compressor, is sent to the combustor, wherein fuel is added for combustion at near constant pressure. The air and fuel mixture in the combustor burns and creates high temperature which then drives the turbine and compressor impeller attached to the turbine shaft. Exhaust then flows through the nozzle at the end of the engine with a very high velocity that produces thrust. The engine is shown in Figure 7.

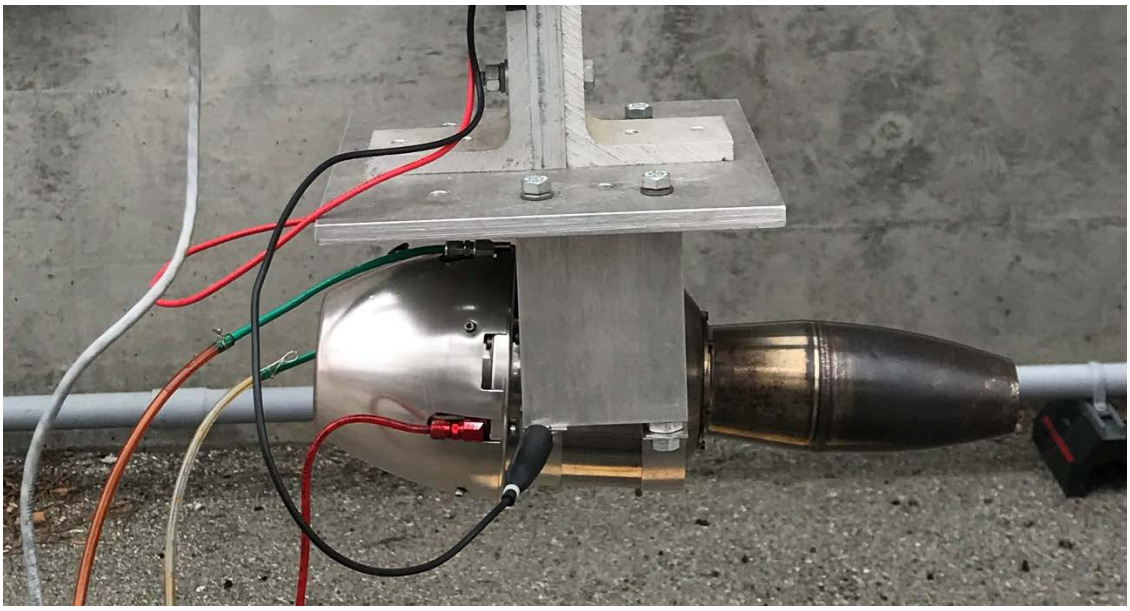

Figure 7. The Sophia Turbojet engine was installed in the outdoor test stand

The Sophia J450 turbojet engine was designed to run on liquid fuel and has only been used with liquid fuel for past NPS theses. This engine is no longer commercially

available but operates within its parameters so offered this project a suitable engine baseline. The engine's specifications are show in Table 1.

Table 1. Sophia J450 turbo engine specifications. Source: [13].

Engine Dimensions	Length = .3536 m (13.19 in) Diameter = .1199 m (4.72 in)
Weight	.454 kg (4 lbs)
Thrust	48.9 N (11lbs) at 123,000 rpm
Exhaust gas temp	704 deg C (1300 deg F) max
Fuel consumption	200 cc/min max
Throttle System	Electronic speed control to fuel pump
Lubrication system	Total loss oil mist system
Starting System	Compressed air
Ignition System	Spark plug
Compressor Pressure Ratio	1.26 bar(18.3 psi) max
Fuel Pressure	2.75 bar (40 psi) max

The engine apparatus was installed outside of the Gas Dynamics Laboratory at the Naval Postgraduate School, Building 216. The apparatus is shown in Figure 8. A 167.6 cm (66 inch) by 10.2 cm (4 in) I-beam was bolted to a concrete wall outside of Building 216. The engine was hung from the I-beam by a spacer, thrust beam, and cradle.

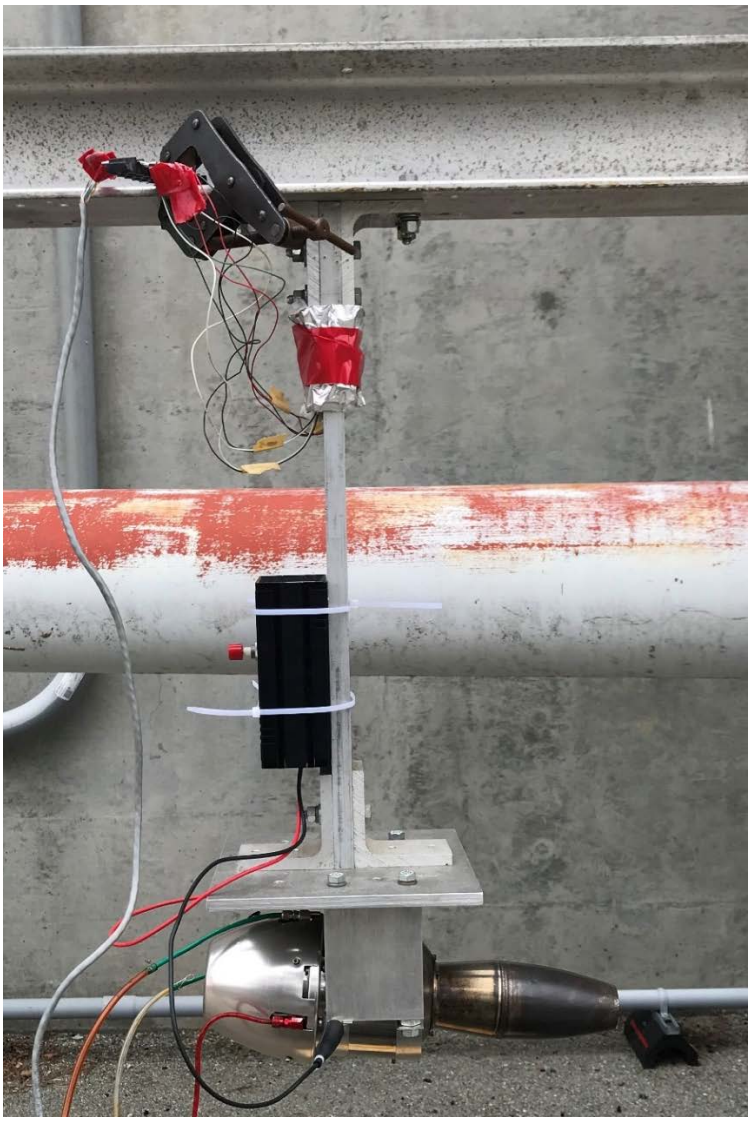

Figure 8. Turbojet engine was attached to an I-beam and cradled at the bottom of the apparatus

2. Capstone Model C30 MicroTurbine

The Capstone C30 MicroTurbine is a high-speed generator powered by a turbine that when coupled with digital-powered electronics, produces electrical power [15]. The microturbine engine is a combustion turbine that includes a compressor, combustor, turbine, generator, and a heat exchanger [15]. A single shaft, supported by air bearings, rotates the C30 MicroTurbine which can reach speeds up to 96,000 rpm. The permanent

magnet generator outputs variable frequency AC that is used to power the start and cool down of the motor [15].

Other features of the C30 MicroTurbine include a “state of the art digital power controller with built-in protective relay functions, patented air bearings that eliminate the need for oil or other liquid lubricants, and an air-cooled design of the entire system that eliminates the need for liquid coolants” [15]. The engine only has one moving part and combined with the innovative combustion control, the C30 MicroTurbine provides extremely low emissions. Figure 9 shows a diagram of the C30 Microturbine parts.

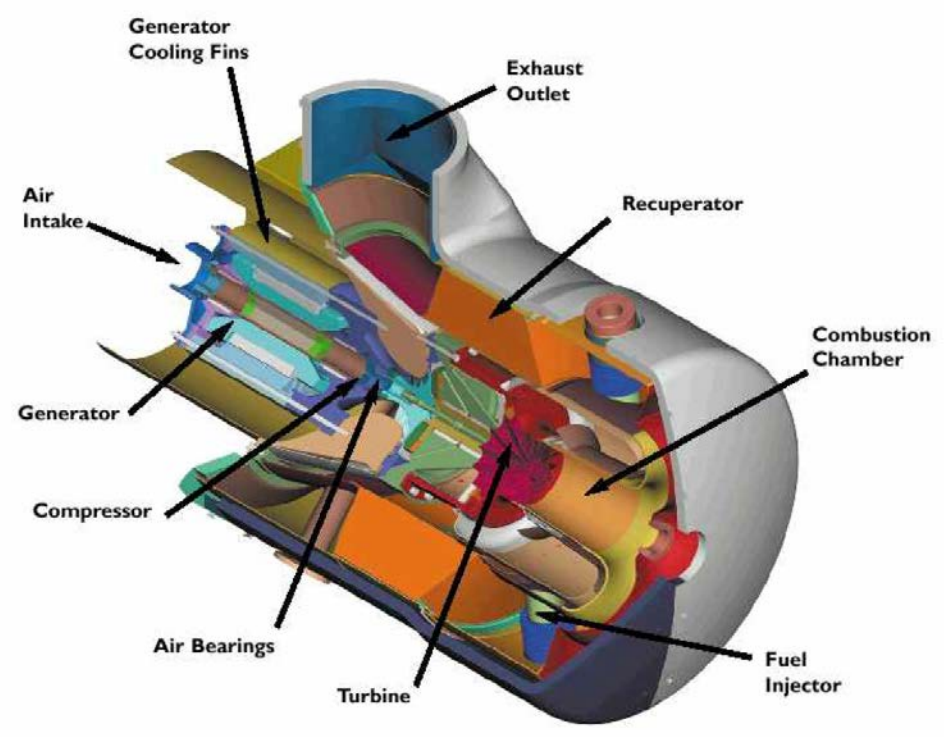

Figure 9. Typical Capstone Model C30 microturbine engine assembly. Source: [15].

The integral annular heat exchanger, or recuperator, helps to double thermal efficiency for the turbine [15]. The new digital control technology makes the MicroTurbine compatible for on-site or remote user interface while providing complete diagnostic capabilities. The design of the C30 MicroTurbine can be paralleled with an electric utility

grid or with another generation source from the AC electrical power output [15]. It is also able to operate in Stand Alone mode for off-grid power or in MultiPac mode, which allows multiple systems to be joined and controlled as a single source. External features and the envelope dimensions of the C30 MicroTurbine are shown in Figure 10.

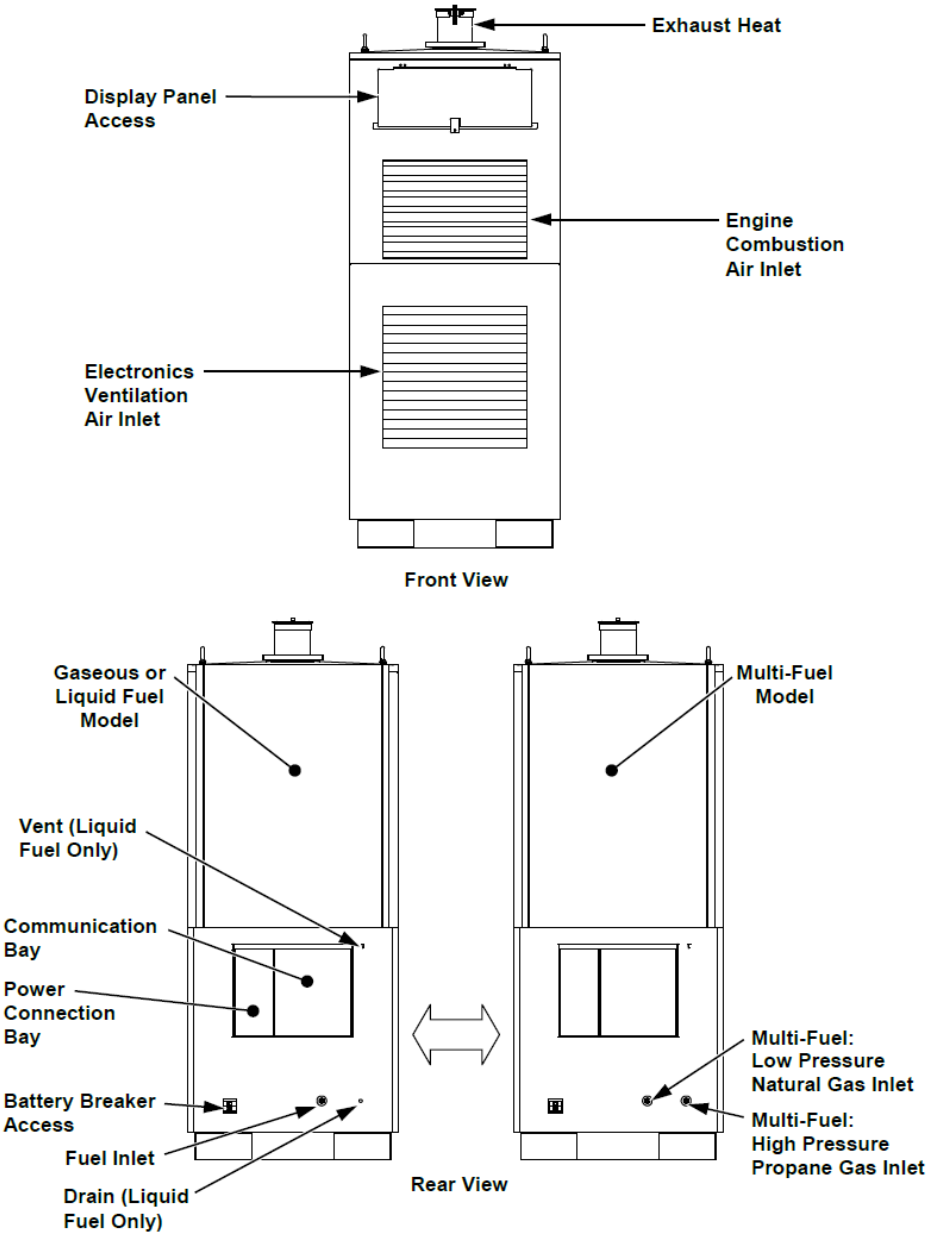

Figure 10. External details of Capstone C30 microturbine design. Source: [15].

For this research, the microturbine will be used in Stand Alone mode. Stand Alone operation is most commonly used to support remote facilities where the normal electric utility grid is unavailable. When disconnected from the grid, the microturbine is supported by a battery pack that stores energy for startup and then provides a buffer during operation for sudden load changes [15]. However, during Stand Alone mode, battery management is automatic with the system designed to keep the battery charged to around 80% during operation and when a user commanded shutdown is initiated, the microturbine will attempt to fully recharge the battery to 90% before it enters cool down and a final shut down [15].

To baseline the microturbine, this research plans to use propane gas to power a 5-kilowatt (kW) load. Through the given specifications of the engine, it is estimated that a 5-gallon (20 lb) propane tank will last approximately 6.5 hours for turbine operation. The math is shown in Equation 1 using the Net Heat Rate LHV of 13,100 Btu/kWh and the conversion rate of 21,591 Btu/lb of propane.

$$20\ lb\ propane\ \left(\frac{21{,}591\ Btu}{1\ lb\ propane}\right)\left(\frac{1\ kWh}{31{,}100\ Btu}\right)\left(\frac{1}{5\ kW\ load}\right) = 6.59\ hour \qquad (1)$$

It is important to understand how the battery operates to understand engine operation. When the engine is started, it will drain the battery, but the battery will charge as the engine operates. To restart the engine from rest, the battery must be charged, and the simplest way to charge the battery is while the engine is operating; thus the propane fuel supply must be able to last long enough for the engine to charge the battery.

B. INSTRUMENTATION

To baseline the Sophia J450 engine, proper operation of the turbojet engine using liquid fuel was vital in order to accurately compare the results to the engine testing using hydrogen gas. A 3 V oil pump was needed with turbine oil shown in Figure 11 to lubricate the engine. A 12 V fuel pump was used to drive fuel to the engine, shown in Figure 12. The fuel pump was set to 12 V and the current was then adjusted to regulate the amount of fuel entering the engine. The liquid fuel used was Coleman fuel which is a mixture of cyclohexane, nonane, octane, heptane, and pentane. Both pumps were powered by power supply boxes in order to be able to readily adjust and easily set each pump to the preferred

output. A standard operating procedure for the turbojet engine operation is given in Appendix A.

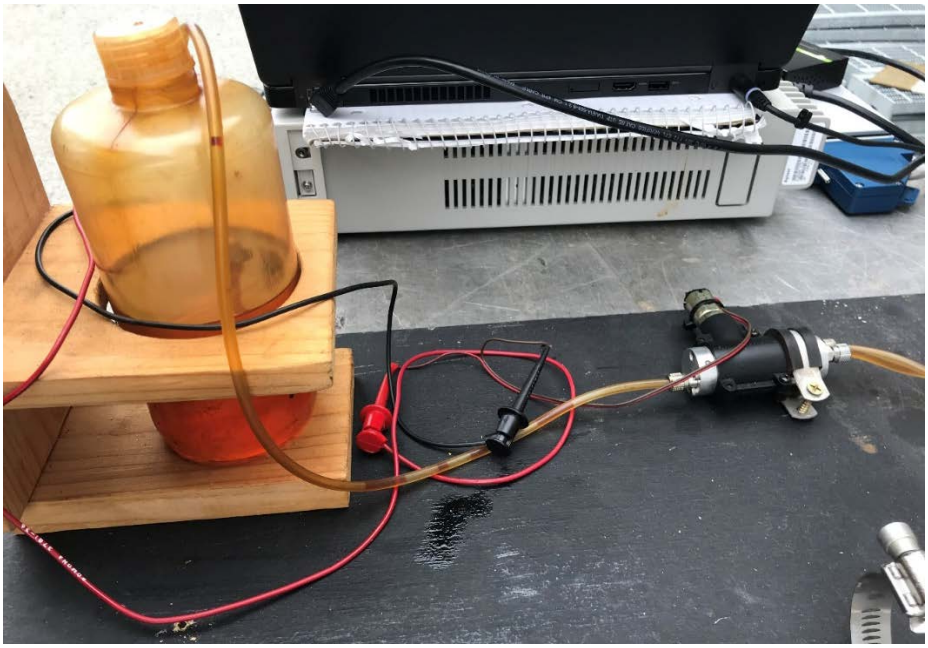

Figure 11. The oil pump used to lubricate the turbojet engine

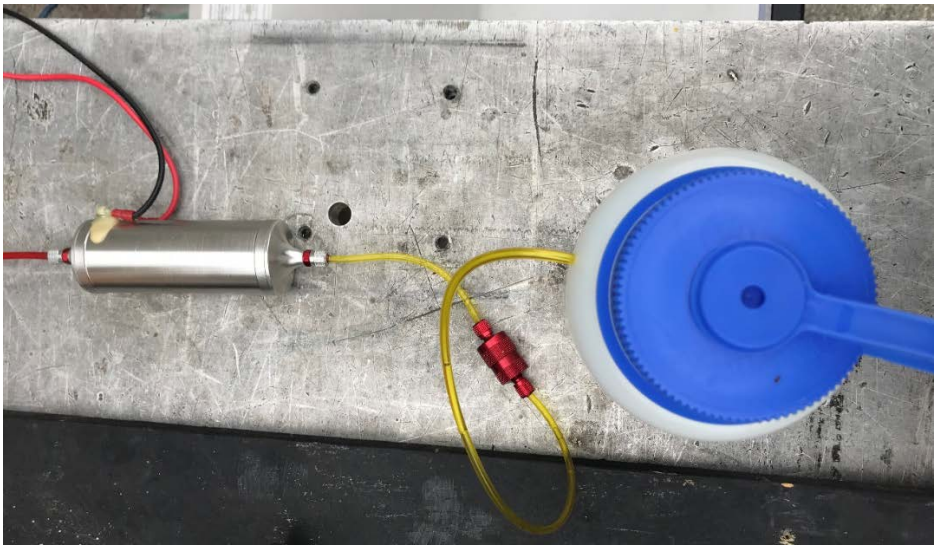

Figure 12. The fuel pump used to supply the engine and powered by an independent power supply

The liquid fuel used was Coleman fuel which is a mixture of cyclohexane, nonane, octane, heptane, and pentane [16]. Coleman white gas has an octane rating of 50 to 55 and a flammability similar to gasoline. White gas has a heating value of approximately 41.617 MJ/kg (17,900 BTU/lb) [16]. Coleman gas is similar to kerosene gas in use, but the individual properties of the two gasses vary greatly and are contrasted in Table 2.

Table 2. Comparison of Coleman gas and kerosene gas properties.

Property	**Coleman Gas**	**Kerosene Gas**
Color	Colorless [a]	Pale Yellow [d]
Boiling Point	98 deg C (208 deg F) [a]	175 deg C (347 deg F) [d]
Flash Point	-4 deg C (24.8 deg F) [a]	38 deg C (100 deg F) [d]
Vapor Pressure	0.365 bar (5.3 psi) [a]	approx. 0.05 bar (0.73 psi) [d]
Density	0.68 kg/m^3 (42.5 lb/ft^3) [a]	0.804 kg/m^3 (50.2 lb/ft^3) [d]
Heating Value	41.6 MJ/kg (17,900 Btu/lb) [f]	46.2 MJ/kg (19,900 Btu/lb) [f]
Viscosity	0.00029 Pa-s (0.000194 lb/ft-sec) [b]	0.00164 Pa-s (0.0011 lb/ft-sec) [c]
Auto ignition Temperature	215 deg C (419 deg F) [a]	210 deg C (410 deg F) [d]

[a] Source: Safety Data Sheet Coleman Fuel, http://www.farnell.com/datasheets/1700915.pdf

[b] Source: Petroleum Naphtha, https://cameochemicals.noaa.gov/chris/PTN.pdf

[c] Source: Dynamic viscosity of common liquids, https://www.engineeringtoolbox.com/absolute-viscosity-liquids-d_1259.html

[e] Source: Material Safety Data Sheet Kerosene, http://www.sciencelab.com/msds.php?msdsId= 924436

[f] Source: Combustion Science and Engineering, p. 851, Annamalai, Kalyan; Ishwar Kanwar Puri, 2006.

Considering these properties and their application helped to understand the results of the liquid fuel engine operation. A lower viscosity of the Coleman gas would allow the fuel to spread quicker and vaporize more than the standard operation of kerosene gas. A lower auto ignition temperature and flash point also help to further explain the results that were generated.

Two pressure gauges were used to measure the inlet fuel pressure and the compressor outlet pressure. The fuel pressure gauge was imperative to ensure the engine was not being flooded with fuel as it was operating. The compressor pressure gauge was critical for baselining the engine operation as the compressor pressure ratio was used to compare the liquid fuel operation to the hydrogen operation. The setup is shown in Figure 13.

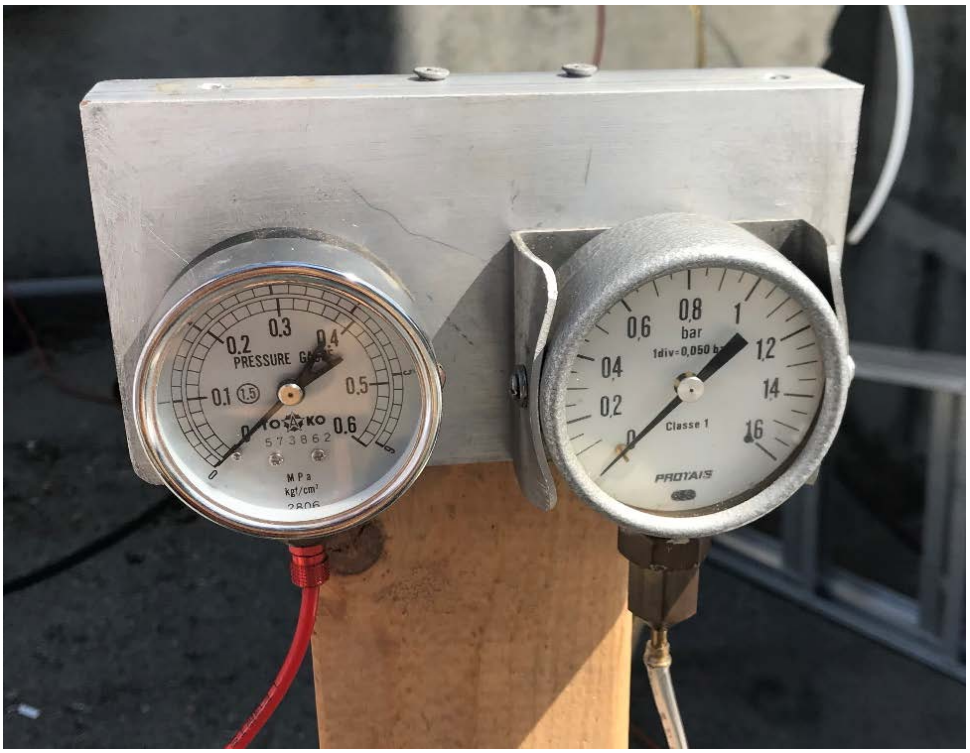

Figure 13. The fuel pressure gauge (left) and the compressor pressure ratio gauge (right) were used to ensure proper operation of the equipment

A National Instruments 9237 module strain gauge was used to calculate thrust and is shown in Figure 14. The device used a full Wheatstone bridge to measure voltage difference across the bridge. Thrust was measured by the deflection of the metal beam from which the engine was suspended. Four strain gauges were applied to provide maximum sensitivity and temperature compensation.

Figure 14. The National Instruments strain gauge measured the voltage across the full Wheatstone bridge

The device measures electrical resistance values by using two series strings in parallel whose resistances are connected between a voltage supply terminal and ground to produce zero voltage difference between the two parallel branches when balanced. The strain gauge was activated using a MATLAB code to determine the maximum voltage over a designated period of time and write the voltage data into a table and a graph. Calibration

of the sensors were taken post engine operation. The MATLAB code to write and plot the data is shown in Appendix B.

C. BASELINE TESTING

Baseline testing of the turbojet engine was critical in order to be able to compare the liquid fuel operation results with the hydrogen gas operation results. Initial results during testing of the turbojet engine using liquid fuel are shown in Table 3.

Table 3. Baseline testing with liquid fuel result data

Fuel Pressure	3.1 bar (44.96 psi)
Compressor Pressure Ratio	1.35 bar (19.58 psi)
Thrust	62.3 N (14 lbs)

The operating parameters given in the Sophia turbojet engine operating manual from Table 1 show that a comparison of the maximum operating parameters and the experimentally tested values were similar. Specifically, the compressor ratio experimental value shows a 6.9% difference and the fuel pressure ratio shows only a 12% difference. The measured thrust value was calculated using relationships between force and voltage and varied 24% difference from the expected max value. The experimental data showed that using Coleman liquid fuel caused the engine to operate above the normal maximum conditions. This was likely the result of the more complete combustion of the liquid fuel that was used during testing.

The strain gauge reading captured the voltage across the Wheatstone bridge and produced the graph in Appendix C. This shows the maximum voltage across the bridge was 0.0057 V while the engine was in operation. Figure 15 shows the raw voltage data converted to thrust based on the post-calibration of the strain gauge device and then plotted. The data continued to collect for a total of two minutes so one can see the gradual increase as the engine started and then dramatic decrease as the engine was stopped.

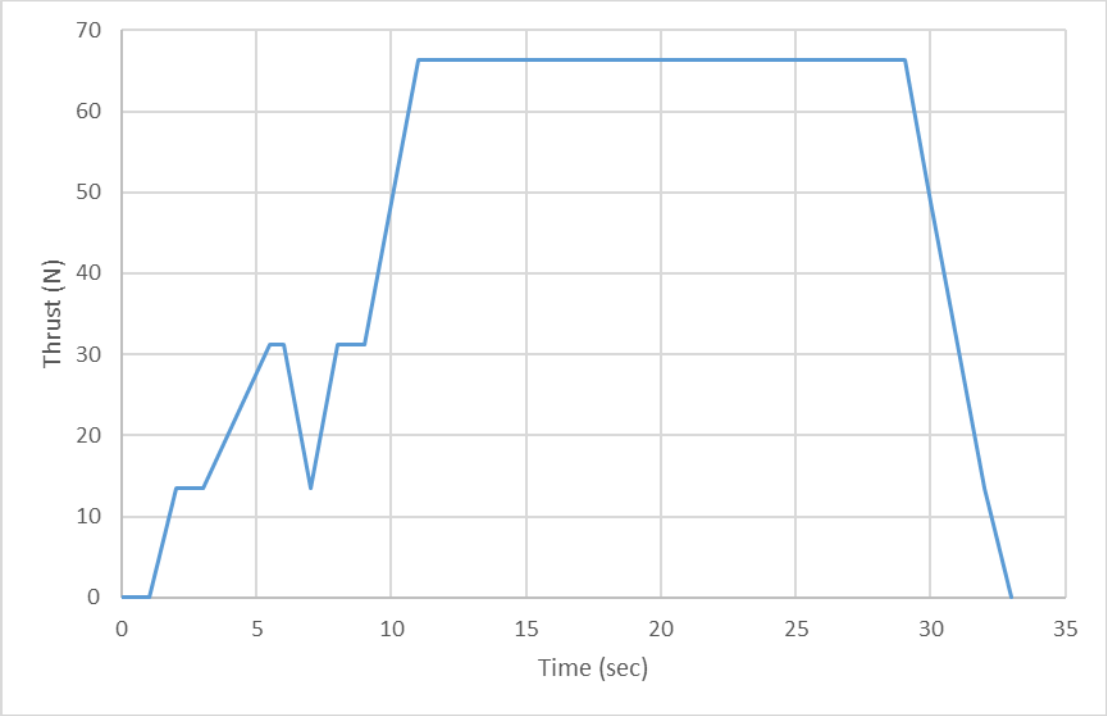

Figure 15. Thrust (N) vs. time graph to measure thrust during experimental liquid fuel turbojet operation

Extrapolating data from prior testing of the Sophia J450 Engine, the experimental thrust value can estimate the speed of the engine. Garcia ran the engine at different speed variations to measure thrust and the specific fuel consumption, so using this data can help to estimate the speed of the turbojet engine [17]. Based on his data, with 62.3 N (14 lbs) of thrust, the Sophia turbojet engine ran at 135,249 rpm. The turbojet engine is specified to operate at 123,000 rpm which is an 9.95% increase from the extrapolated test speed. The Excel extrapolation is shown in Appendix D. The engine operated over the maximum parameters and it can be reasoned that the fuel type played a large factor in the results. The liquid fuel used has a lower viscosity and lower flash point which causes the fuel to vaporize more and ignite easier inside the engine, causing it to over speed.

This proved the turbojet engine was operating normally and with ideal parameters using liquid fuel. Knowing the turbojet engine operating baseline, then the results produced operating with hydrogen would show any variation in performance.

III. HYDROGEN TESTING

A. EXPECTATIONS

Running the turbojet engine with hydrogen gas required advanced safety measures and an experimental setup. With the assistance of the Rocket Laboratory at the Naval Postgraduate School, the turbojet engine was safely enclosed in a test cell to ensure safety of the observers from combustion effects or possible damage to the engine. The Rocket Laboratory commonly uses hydrogen for their combustion research, so creating a new design for hydrogen flow from storage cylinders to the engine was not needed for this stage of the research.

Ideally, running the turbojet engine off of hydrogen would warrant the same or better performance of the turbojet engine. The variables compared were thrust and compressor ratio. With these two parameters successfully found during experimental testing using liquid fuel, comparing these values would show if hydrogen gas allowed the engine to perform as expected. With the added goal to improve gas turbine efficiency using hydrogen gas to fuel a turbojet engine, it was expected that hydrogen gas would allow the engine to operate at the same or better operating parameters. It was also anticipated that the hydrogen gas would cause the engine to over speed, which would then alert the operator to stop hydrogen fuel flow to the engine.

Gasturb was used to calculate the flow rate of hydrogen in the turbojet. Using settings to replicate the turbojet engine, a flow rate of 0.0004 kg/s (0.0009 lbs/s) was found with a compressor ratio of 2:1, which would make the expected pressure of the combustion chamber to be around 2.068 bar (30 psi). Further details of the Gasturb calculations are shown in Appendix E.

B. SYSTEM CONFIGURATION

1. Hydrogen Piping

The hydrogen piping used for the engine operation was already in place because the Rocket Propulsion Laboratory at Naval Postgraduate School regularly uses hydrogen

for their experiments. Using the existing hydrogen piping made programming and the test cell set up easier. The hydrogen system was comprised of the hydrogen supply, Figure 16, a ball valve, Figure 17, a regulator, and another valve with a pressure gauge, Figure 18, before connecting to the engine.

Figure 16. The hydrogen supply was outside the test cell and was piped into the cell through this system

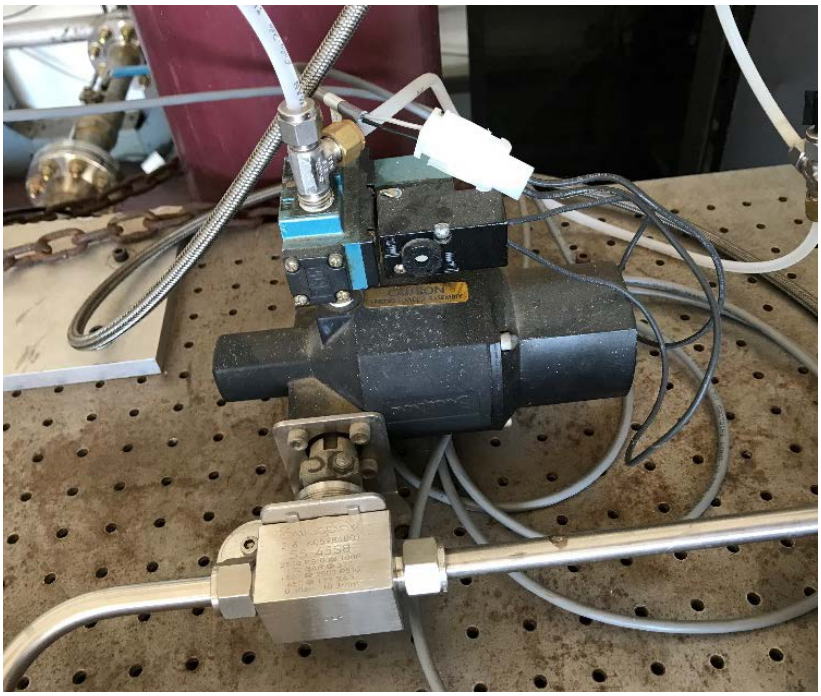

Figure 17. Hydrogen ball valve to control hydrogen flow

Figure 18. Hydrogen supply valve with associated pressure gauge to read the pressure supplied into the engine

Tygon tubing was used to connect the steel hydrogen piping to the engine. Because the engine fuel injector required such small diameter tubing, 6.35 mm (1/4 inch) Tygon tubing was swaged to the hard line and an adapter connected the Tygon tubing to the plastic tubing into the engine, as seen in Figure 19.

Figure 19. The hydrogen tubing from the steel line into the engine

2. Engine Test Configuration

A schematic of the test cell for the turbojet operation using hydrogen is shown in Figure 20. It includes all of the major equipment and a general layout of the test cell.

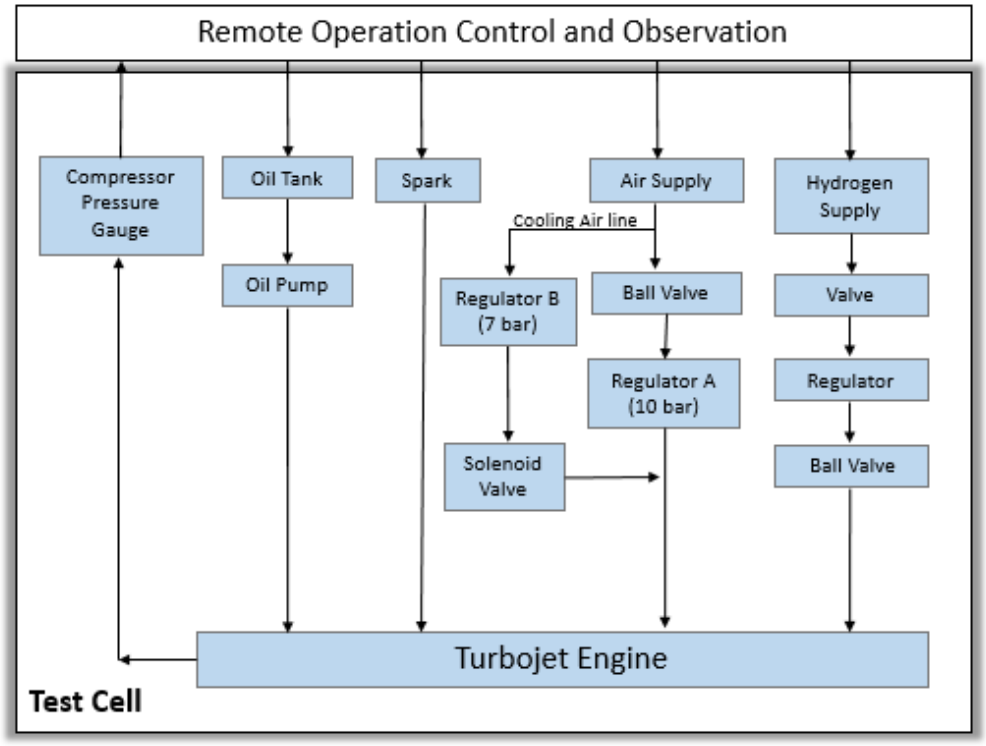

Figure 20. Test cell schematic for hydrogen testing

For safety reasons, all operators and observers were to be out of the test cell during operation which meant that all equipment had to be operated remotely. The oil pump, 10.13 bar (150 psi) air supply, and spark ignition were all activated remotely using the same instrumentation from the liquid fuel run that was modified to operate remotely. A small hole was drilled into the top of the engine combustion chamber housing to aid in the release of hydrogen gas buildup. The hole was designed as an extra safety measure to not disturb the combustion process, but to prevent a large combustion and possible engine damage due to excess hydrogen in the engine.

The engine was mounted on the bread-board table in the test cell, as shown in Figure 21. The oil and spark were connected using the same piping and connection system as in the liquid fuel run but with relays added to each component so that they could be properly commanded remotely and turned off if necessary for the safety of the equipment.

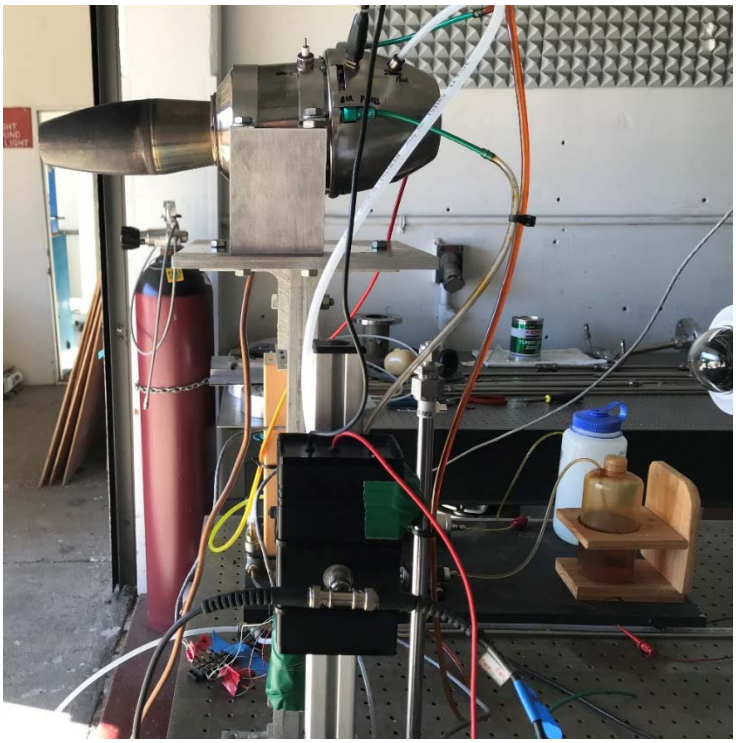

Figure 21. The engine apparatus mounted in the test cell

Before hydrogen testing, the engine was testing using liquid fuel to ensure that the oil pump, start air, spark, and cooling air were all operating correctly. This liquid fuel testing results proved to be the same as the initial testing by comparing the compressor ratios.

3. Turbine Sensors and Support Systems

The initial test using liquid fuel ensured proper operation of the remote equipment set up test cell. The spark was modified from a push button to an outlet that could be connected to a relay, shown in Figure 22.

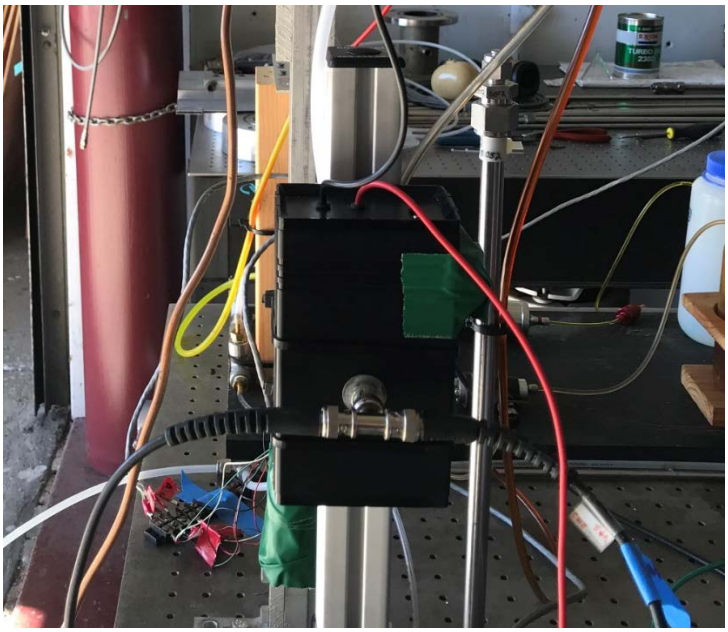

Figure 22. The spark used for combustion

The oil pump power supply was connected to a relay so that when that relay was signaled to turn on, the power supply would turn on at the exact voltage and needed to immediately power the pump, shown in Figure 23.

Figure 23. Oil pump power supply connected to relay to remotely start the pump

All of the same wiring and piping used during the liquid fuel experiment were used again during the hydrogen testing with the piping connected to the engine and secured away from the engine intake, as seen in Figure 24.

Figure 24. Piping configuration into the engine apparatus

The compressor pressure was measured using a 2.1 bar (30 psig) pressure transducer. It was also connected locally to a pressure gauge with a camera set to view the gauge in order to ensure the readings were accurate. Figure 25 shows the transducer was also connected to a relay so that it could be displayed remotely in the control room.

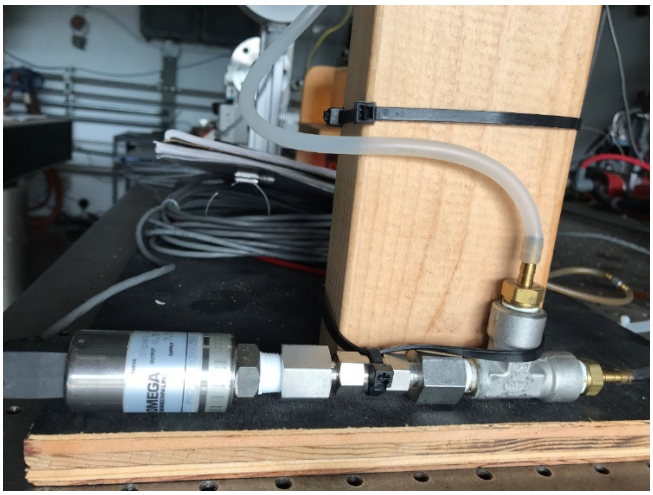

Figure 25. Pressure transducer connecting the relay, a pressure gauge, and to the engine piping

Air supply had two different lines that provided start and cooling air. Start air was regulated from to 10.3 bar (150 psi) after passing through a ball valve, as shown in Figure 26. The cooling air was regulated to 6.89 bar (100 psi) and then passed through a solenoid valve, as seen in Figure 27. These two lines were connected with a tee-connector to feed the Tygon tubing used for air injection.

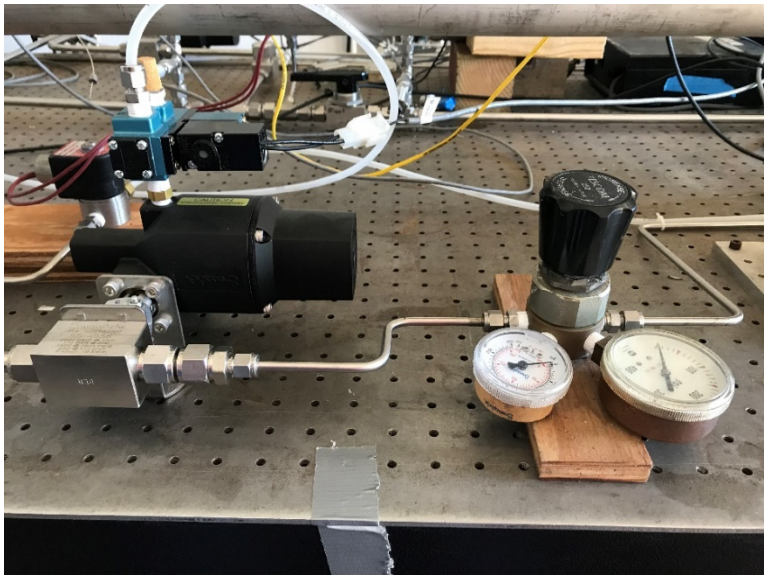

Figure 26. The start air ball valve and pressure regulator system

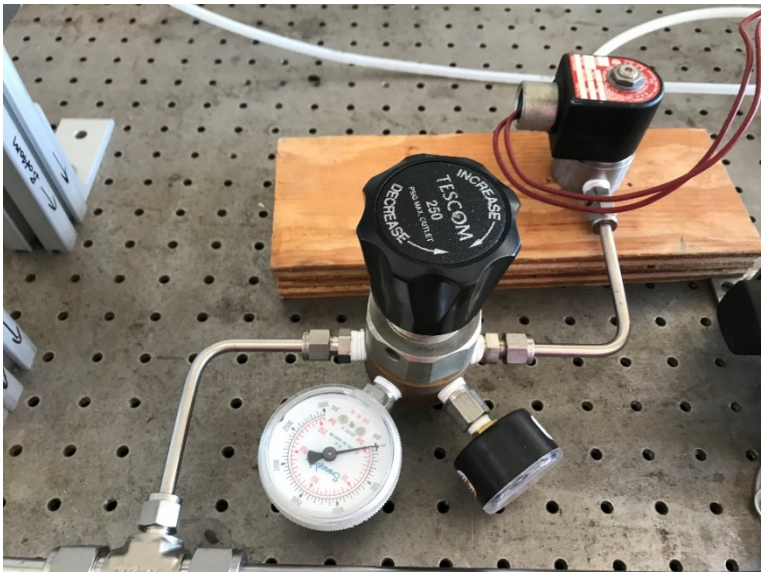

Figure 27. The cooling air pressure regulator and solenoid valve system

The hydrogen had two main pressure gauges throughout the piping system. One transducer read the supply hydrogen pressure while the next one in the piping measured the pressure flowing into the engine after the ball valve that were previously discussed.

Thermocouples were also added on the combustion chamber housing and in the exhaust flow. Since the engine could not visibly be seen rotating and the changes in speed were often difficult to distinguish in the remote observation center, the thermos couples were added to be able to verify that combustion was occurring by noting the temperature changes throughout the run.

4. Testing

After verifying the alignment and all piping for leaks, LABVIEW was used to create an operating sequence to automatically run through each service to the engine. It was also created so that the hydrogen supply pressure could be manually adjusted throughout the run if needed. The sequence used in LABVIEW was similar to the liquid fuel verification test that we used but with the added hydrogen component. Before starting testing, the engine was always manually primed with oil to ensure proper bearing lubrication. First sent to the engine was the oil, then the start air and spark were simultaneously added. After about 2 seconds, the hydrogen was sent to the engine. There were two conditional statements within the sequence code: the first to turn off the start air and spark when the compressor pressure reached .28 bar (4 psig) and the second was a safety to abort the engine run if the compressor pressure reached .8 bar (11.8 psi). The abort conditional was to ensure that the engine was protected and was not over sped.

Gasturb calculations based on wanting a 0.0004 kg/s (0.00088 lb/s) flow rate of hydrogen into the engine, it was estimated that the hydrogen supply line would need a .00132 m (0.052 inch) choke. This choke was inserted into the line between the hard line and Tygon tubing into the engine. Initially, the hydrogen supply pressure was set to 6.55 bar (95 psig) but this low pressure did not show any sign of light off within the engine. Next, starting at 8.27 bar (120 psig) and incrementally increasing to 13.78 bar (200 psig), the compressor pressure steadied at 0.31 bar (4.5 psig). From this reaction, it was assumed

that the flow was not being choked enough and that not enough back pressure was being created to fill all of the fuel injector nozzles.

Because choked flow was in question, the choke within the flow was tested at 6.89 bar (100 psi) and it was determined that the flow through the orifice was not choked because the fuel nozzle orifice size was too small comparatively. The orifice within the flow was then removed and the piping was retested for leaks. For the next round of testing, a conditional statement was added to turn off spark and start air at a compressor pressure of 0.27 bar (4 psig). Thermocouple sensors were added to the engine combustion housing and downstream of the exhaust to be able to gather temperature data and ensure combustion was occurring. The run time was also increased from the initial estimate of 10 seconds to 15 seconds in order to allow time for the user to incrementally increase hydrogen pressure and for combustion to fully develop. Appendix F gives the standard operating procedure for hydrogen testing.

THIS PAGE INTENTIONALLY LEFT BLANK

IV. RESULTS AND DISCUSSION

A. RESULTS

The successful run operated initially at 20.68 bar (300 psi) hydrogen supply with a conditional statement that had the start air and spark turn off when the compressor pressure reached 0.27 bar (4 psig). At that point, hydrogen supply was increased to 27.5 bar (400 psi) which increased the compressor ratio to approximately 0.41 bar (6 psig). With a slight drop in compressor pressure to almost 0.31 bar (4.5 psi), but then a steady increase to 0.50 bar (7.3 psig), the compressor pressure held steady until the cooling sequence was initiated. With the maximum compressor ratio at 1.26 bar (18.3 psig), and witnessing that the compressor ratio reached 0.50 bar (7.3 psig) and held steady until cooling started, the run was deemed to successfully operate at about 85.3% speed at 98,140 rpm. The total run time of the engine was 15 seconds.

From the successful run that steadied at a compressor pressure of 0.50 bar (7.3 psig), the following charts were produced graphing the hydrogen pressure into the engine, Figure 28, the compressor pressure, Figure 29, the external temperature of the combustion housing, Figure 30, and the temperature of the exhaust flow, Figure 31.

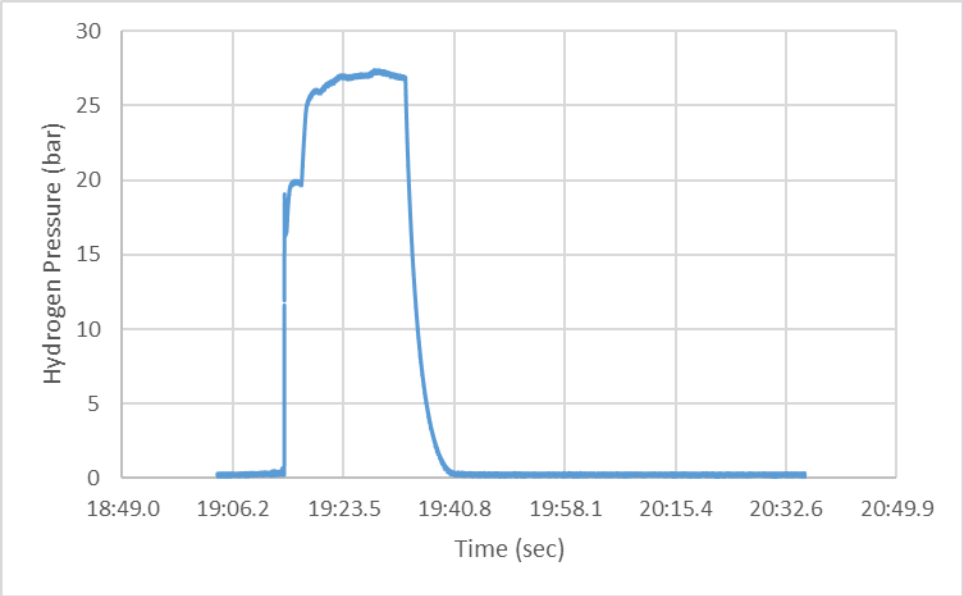

Figure 28. Hydrogen supply pressure into the engine

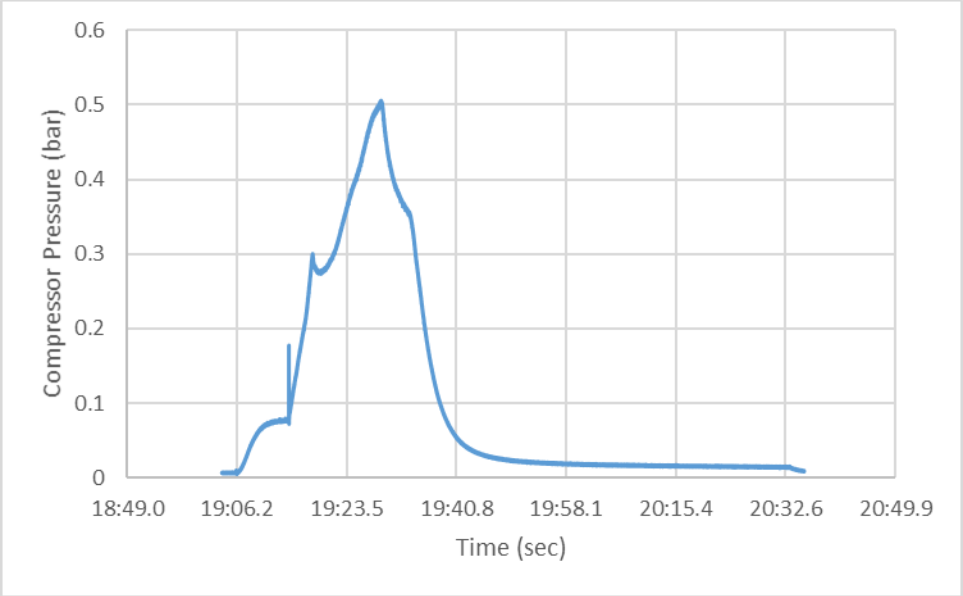

Figure 29. Compressor pressure throughout hydrogen experiment

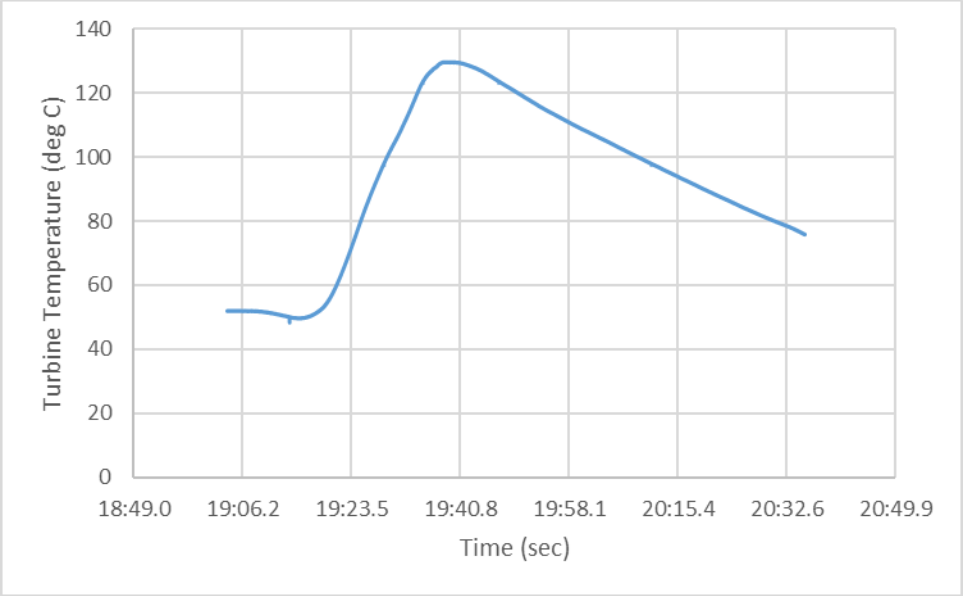

Figure 30. Temperature of the combustion chamber housing

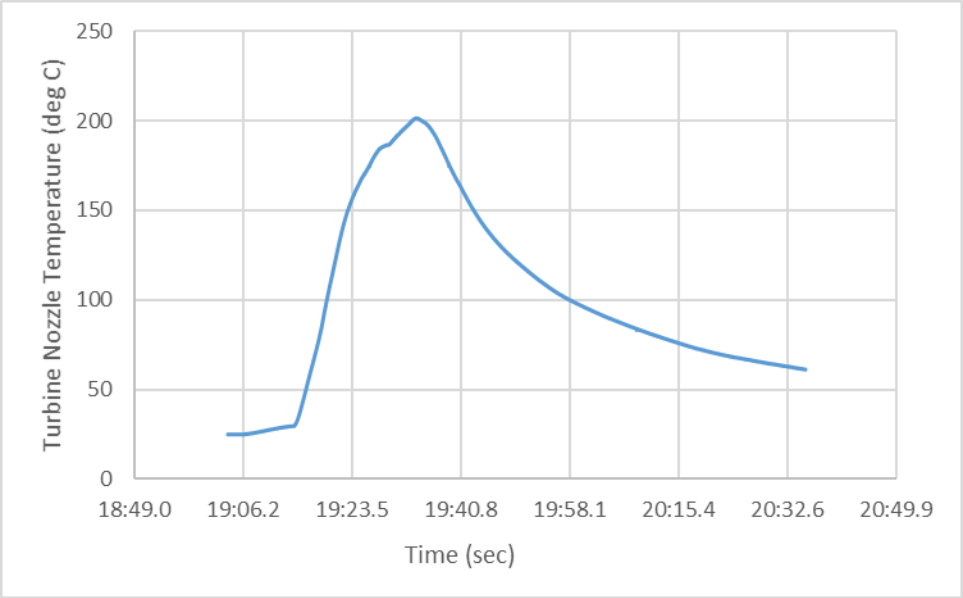

Figure 31. Temperature of the exhaust flow

These charts show the incremental increase of the hydrogen supply pressure and how each increment increase effected the compressor pressure. The compressor pressure graph shows the peak of 0.50 bar (7.3 psig) before the cooling system initiated after the 15 second run time. The smaller peaks on the compressor pressure graph represent the slow

combustion of the engine as the pressure was incrementally increased. The temperature graphs confirm that the maximum combustion temperature was 129.8 deg C (265.6 deg F) and the maximum exhaust temperature was 201.5 deg C (394.7 deg F).

The thrust measurements were scaled compared to the results taken from the liquid fuel run. The thrust graph produced in the hydrogen run is shown in Figure 32. The first peak in Figure 32 represents the initial light off of the hydrogen fuel and the final peak is the continued full combustion as the compressor pressure increased until the cooling sequence initiated. It is believed that before enough back pressure was created to fill all 10 fuel nozzles, only partial combustion was taking place which is represented with the initial peak.

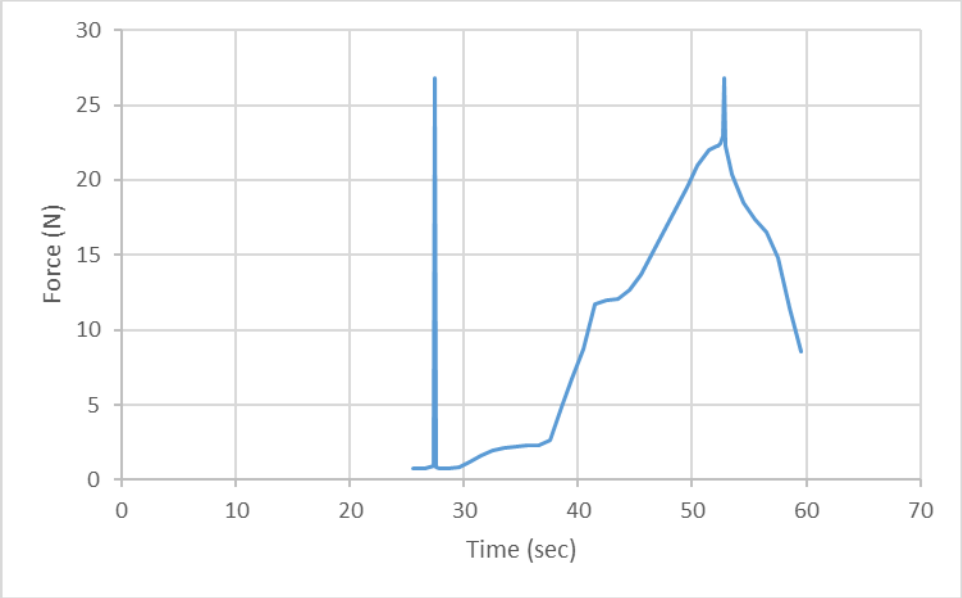

Figure 32. Thrust (N) vs. time graph to measure force during experimental hydrogen turbojet operation

B. ANALYSIS

Though the successful hydrogen test run did not reach maximum speed, multiple facets of data can be taken to analyze the hydrogen combustion and understand future engine operation using hydrogen as the only fuel source. The hydrogen fuel mass flow rate can be calculated assuming the fuel nozzles were choked and knowing the diameter of each

fuel nozzle orifice to be 1.27x10^{-8} m^2 (0.005 inch), there were 10 nozzles, the upstream pressure of 27.5 bar (400 psig), and the downstream pressure of 0.5 bar (7.3 psig). Thermodynamic tables characterizing one-dimensional isentropic compressible flow for an ideal gas with constant specific heat [18] can be used to further specify the choked flow and using the following calculations, the fuel mass flow rate can be found.

$$\rho^* = \frac{P^*}{RT^*} = \frac{1456224\ Pa}{\left(4124.3\frac{J}{kg*K}\right)(211\ K)} = 1.447\frac{kg}{m^3}$$

$$A = \frac{\pi d^2}{4} = \frac{\pi * (0.000127m)^2}{4} = 1.2667\ x\ 10^{-8}\ m^2$$

$$V = \sqrt{kRT} = \sqrt{(1.409)\left(4124.3\frac{J}{kg*K}\right)(211\ K)} = 1190.76\frac{m}{s}$$

$$\dot{m} = \rho AV = \left(1.447\frac{kg}{m^3}\right)(1.2667\ x\ 10^{-8}m^2)\left(1190.76\frac{m}{s}\right) = 0.0000218\frac{kg}{s}$$

$$\dot{m}_{total} = \dot{m} * 10\ nozzles = 0.0000218\frac{kg}{s} * 10 = 0.000218\frac{kg}{s}$$

Using those values, the fuel rate for one fuel nozzle was found to be .0000218 kg/s (0.0000481 lb/s) so entering the combustion chamber through the 10 nozzles was 0.000218 kg/s (0.00048 lb/s) of hydrogen. Compared to the expected 0.0004 kg/s (0.0009 lbs/s), the actual mass flow rate was almost half. The lower mass flow rate could explain the extremely high pressures that were needed to create enough back pressure for the fuel nozzles and provoke combustion during testing.

The direction of the strain graph in Appendix C compared to the liquid fuel raw voltage results is opposite due to the direction that the mount and the direction the engine was mounted. However, these graphs can be scaled by taking the difference between the peak and the zero as shown in Figure 15 and Figure 32. The liquid fuel run showed a 0.00035 volts difference between the voltage peak and its zero which equated to 62.3 N (14 lb) of thrust. Comparatively, the hydrogen thrust graph showed a difference of 0.00013 volts which shows that the engine produced approximately 43% the amount of thrust running off hydrogen at 72% speed compared to the liquid fuel at 118% speed. This results

in estimating that the hydrogen run produced approximately 26.7 N (6 lbs) of thrust. Appendix G shows the Gasturb calculations using off design predictions and the 26.7 N (6 lbs) of thrust, it is deducted that the specific fuel consumption is approximately 0.0014 N/kg*s (0.51 lb/lbm*h).

Using the same extrapolation method shown in Appendix D to determine the thrust measured during the liquid fuel run, it was possible to determine the predicted speed of the engine. The estimated 26.82 N (6 lbs) of thrust predicted the engine was rotating at 98,140 rpm, which is 85.3% of the maximum speed of 115,000 rpm and 72.5% of the extrapolated speed during the liquid fuel testing, 135,249 rpm. Although the measured thrust produced using hydrogen is only 43% of the thrust produced using liquid fuel, the estimated speed at which the engine was rotating is a logical estimate due the engine not being at complete combustion before the run was interrupted by the cooling cycle which would create a lower thrust. The mixture of hydrogen and air coupled with the properties of hydrogen molecules would also explain the high speeds of the turbine without producing the same ratio of thrust. The thrust found from the hydrogen run was compared and substantiated using the strain data from the liquid fuel run. The liquid fuel run produced a steady thrust reading, and thus more reliable reading to base thrust data produced during the hydrogen fuel run.

The reaction of hydrogen in the engine compared to the liquid fuel may be linked to the comparison of the stoichiometric flame temperature. Hydrogen's flame temperature is 2210 deg C (4010 deg F) [19] vice kerosene's flame temperature is 2093 deg C (3799 deg F) [20]. The difference in these temperatures can explain possibly the high temperatures experienced inside the combustion chamber. The higher stoichiometric flame temperature of hydrogen allows for higher pressure within the chamber which creates more force in the engine since the process is constant volume. Continuously running a standard turbojet engine using a fuel with a higher stoichiometric flame temperature would eventually melt the combustion chamber because most engine parts are not built to withstand continuous exposure to such higher temperatures and pressures. The difference in the stoichiometric flame temperature between hydrogen and kerosene would affect the analysis of the estimated speed of the engine. Because all of the baseline data is based on

testing using liquid fuel, the interpretation of the hydrogen testing data must also be confirmed and estimated using Gasturb.

To verify the thrust measurement, Gasturb was used to model the expectation of hydrogen testing. Knowing that there was about 99 deg C (211 deg F) difference between the adiabatic flame temperatures between hydrogen and kerosene gas, that difference can be used to anticipate what the 100% model of hydrogen testing would have been. Iterating the burner exit temperature for generic fuel to produce 62.3 N (14 lb) of thrust resulted in a burner exit temperature of 1383 deg K (2490 deg R). Assuming an adiabatic flame temperature difference of approximately 99 deg C (211 deg F), the burner exit temperature was increased to 1755 K (3160 deg R) and fuel source changed to hydrogen. This estimated 75.7 N (17 lb) of thrust when modeled at 100% operation, shown in Appendix G. Since the engine was estimated to be running at 85% of the maximum speed, then 85% of the predicted 75.7 N (17 lb) of thrust would be estimated to 64.3 N (14.45 lb) of thrust. Thus, the maximum thrust experienced during the liquid fuel when the engine over sped is approximately the same amount of thrust experienced when running with hydrogen fuel at 85% speed. Gasturb also predicted that the 100% model using hydrogen gas would produce 0.00192 N/kg*s (0.7042 lb/lbm*h) thrust specific fuel consumption. Operating at the 85% speed during testing, the hydrogen fuel would be predicted to produce a specific fuel consumption of 0.00163 N/kg*s (0.006 lb/lbm*h) which is similar the Gasturb off design predictions and the 26.7 N (6 lbs) of thrust that projected that the specific fuel consumption was approximately 0.0014 N/kg*s (0.51 lb/lbm*h), shown in Appendix H.

Although this testing was successful, issues from prolonged exposure to the higher temperatures and higher pressures inside of the turbine engine can cause failure or damage to the engine. These issues could be avoided with modifications to the turbine including changing the fuel nozzle orifice size and ensuring the metals within the engine can withstand the higher temperatures and higher pressures.

During testing, it was discovered that the fuel nozzle orifice was so small, that the upstream flow would not choke in order to get a proper flow through the fuel nozzles. With the upstream flow not choked, it caused hydrogen to be fed into the engine at much higher pressures than the engine was designed to handle. The higher pressures must also be

monitored to ensure that the bearings and seals throughout the engine design are considered to be able to withstand the increased operating conditions.

Further, with the increase in pressure, there was also a significant increase in temperature within the engine. With the hydrogen adiabatic flame temperature significantly higher than liquid fuel, the temperature of combustion was higher as well. The higher temperatures could cause damage to the internal housing if the metal material reached close to its melting point. Additionally, extended exposure to the abnormal conditions may wear the metals and cause damage or failure of the engine. It would be recommended that if operating under higher temperatures and higher pressures without making modifications to the engine that the engine be allowed to cool and recover from abnormal testing conditions before continuing. Further testing under high pressures caused damage to the engine but it was believed that these modifications would have made the engine more robust and able to withstand extending testing.

V. CONCLUSION AND FUTURE WORK

A. CONCLUSION

Overall, running a turbojet engine with hydrogen gas was successful. The purpose of this research was to determine whether using hydrogen gas to power a turbojet combustion engine was feasible and although there were issues, it was determined that it is plausible to operate a turbojet engine using hydrogen gas. Reaching a steady 0.50 bar (7.33 psi) before the cooling sequence was activated proved that the engine was operating at about 85.3% speed. Although prolonged use of an unmodified turbojet engine using hydrogen gas as fuel would be challenging, the engine test sequence was demonstrated to be robust and able to operate soundly under abnormal conditions. This level of thrust and speed produced using hydrogen without making design modifications to the original Sophia J450 turbojet engine proves that turbojet engine operation using hydrogen could create further future research developments.

B. RECOMMENDATIONS

Further testing using turbojet engines would possibly need modification due to issues that were experienced during testing. The main issues involved the design of the turbojet engine and the high pressure required to obtain results. Because the fuel nozzles inside the turbojet engine were so small and designed to atomize liquid fuel, it caused the need for much higher pressures supplied to the engine than anticipated. If further testing involving a turbojet engine were to take place, possible modification to the fuel nozzles by increasing the orifice size might help. A larger orifice size would allow for the flow to be choked further upstream and not as much need for such high pressures to be fed inside the engine. These high pressures inside the engine also increased the internal temperature of the engine. A possible modification to the turbojet engine would be the need to modify the internal metal material to ensure that the materials throughout the turbine could withstand the higher turbine inlet temperatures. Prolonged exposure to the higher pressures and temperatures would have an effect on the materials inside the engine and could result in failure or damage to the engine.

These two issues aside, the turbine operation was successful. This research serves as the basis for a larger project to create portable hydrogen-powered microgrid for the DoN. Directly applying this research and lessons to running turbines using hydrogen could result in operating a turbine with higher efficiencies with extremely low toxic emissions.

C. FUTURE WORK

This research paves the way for further advancements using hydrogen gas to power engines, specifically further work with gas turbines. To this point, there have been substantial developments made in terms of hydrogen generation and storage. However, further work is needed to progress safe hydrogen use and transport. The next step in this project is to run a Capstone C30 microturbine engine remotely off hydrogen. The smallest microturbine, the Capstone C30, was selected due to its size and the microturbine is already designed to run off gaseous fuel. This microturbine was designed to run off gaseous fuels and will be baselined using propane gas. Because this engine is designed for gaseous fuels, it should have less issues regarding back pressure and fuel nozzle design than when running the turbojet engine using hydrogen gas. Baselining the engine using propane gas will allow the user to compare how efficiently the Capstone C30 runs off hydrogen.

To that end, a C30 engine was successfully run on propane gas for 25 minutes. With no load on the system, the energy produced charged the battery from 72% to 94% before the engine was commanded off using normal shutdown procedures. There is a digital panel on the outside of the engine that allows the user to scroll through and verify different data readings throughout the engine operation. The engine was run steadily at approximately 45,000 rpm and reached a turbine exit temperature of 671 deg C (1240 deg F) before shutdown and cool down sequence was initiated. This success was a catalyst in the process in order to safely run the engine safely off hydrogen. Figure 33 shows the C30 engine with the front panel removed during testing to ensure proper operation of the engine.

Figure 33. The C30 Capstone engine successfully run off propane gas

Using the Capstone C30 specifications, the hydrogen fuel flow characteristics could be determined. A fuel delivery requirement of 0.0014 kg/s (0.003 lb/s) will be used for the hydrogen design with an expected efficiency of around 18–25% [13]. Using a similar replica of the system that was used to operate the turbojet engine with hydrogen should result in a successful microturbine run using hydrogen. Successfully operating the Capstone C30 microturbine using hydrogen gives NPS a starting point in designing a hydrogen energy station and allows the Department of the Navy to potentially harness that energy to efficiently generate electricity while limiting toxic emissions.

The ultimate goal of the project is to create a portable hydrogen-powered microgrid that can be used to generate, store, and use hydrogen safely and efficiently. This potential would allow the DoD to create their own renewable energy powered microgrid that provides a reliable energy source for all conditions, even remote and expeditionary locations.

THIS PAGE INTENTIONALLY LEFT BLANK

APPENDIX A. LIQUID FUEL STANDARD OPERATING PROCEDURE

This procedure was adapted from the Sophia J450 Turbine Engine Instruction Manual and Owners Guide [14].

1. Connect oil pump wiring to remote 12 Volt power supply box prior to engine operation.
2. Connect the fuel pump wiring to a remote power supply box.
3. Connect the air tubing to the engine. Check for leaks in the air supply connection; any leakage or a poor connection may not allow satisfactory rotation.
4. Ensure the spark plug is operating properly by testing and verifying that an adequate spark is produced.
5. Fill the oil tank with standard turbine oil. Fill the fuel tank with Coleman kerosene gas.
6. For the oil pump: Adjust the voltage of the power supply until the oil pump is running consistently. Ensure oil has reached the engine for at least 2–4 seconds before the engine is started to prime the engine.
7. Start air flow through the engine at 10.3 bar (150 psi).
8. Switch the spark igniter to on by pushing the red button on top of the ignitor, spark will occur. A crackling sound should be heard to indicated spark is occurring.
9. For the fuel pump: Set the fuel pump power supply to 12 Volts and adjust the current slowly until the fuel is flowing to the engine.
10. Once fuel has reached the engine, the spark should ignite, and the engine will start. The sound of rotation gradually becomes higher responding to the rotor rpm.
11. The turbine rotation sound level should be very high. If the sound level is not high or if you hear an abnormal sound, stop the engine immediately.

12. After combustion starts, continue the air supply until the compressor pressure is over .3 kg/cm2 (4.2 psi) on the compressor pressure gauge, then release the red button of the ignitor and stop supplying starting air.
13. If the engine does not start within 10 seconds, turn off fuel pump and cease air and spark. Then drain excess fuel from inside of engine by holding engine vertical. Fuel can also be flushed from the system by keeping oil on and running the air through the engine.
14. Confirm the flow lubrication oil are normal while operating. For maximum output, increase the fuel pressure to 2.8 kg/cm2 (40 psi) and compressor pressure to 1.3 kg/cm2 (18 psi). The rpm at this state is about 123,000 rpm, and the thrust is over 11 lbs.
    a. Never exceed 1.3 kg/cm2 (18.3 psi) compressor ratio. This is regulated by the supply of fuel to the engine. Decrease the fuel pressure to decrease the compressor ratio.
15. The engine can be operated for about 5 minutes at this maximum output.
16. To stop the engine operation, cut the power to the fuel pump power supply. If at any time, the fuel or lubrication oil is completely consumed, cut power to the fuel pump immediately.
17. If a long flame blows out the tail pipe, fire in the fuel system area, breakage in the engine, or leakage of the piping, stop the engine immediately by cutting power to the fuel pump, and extinguish is necessary.
18. The engine remains hot for about 1 hour after stopping. Take care when handling.
19. After running, disconnect power to the fuel pump.

APPENDIX B. STRAIN GAUGE MATLAB CODE

```
%NI 9237 Strain Module Connection and Test
close all
clc

%Create the DAQ Station
devices = daq.getDevices;
s = daq.createSession('ni');

%Add Strain Gauge Modules to measure strain
%Only connected for ai0 port
addAnalogInputChannel(s,'cDAQ9181-1D56450Mod1', 0,
'Bridge');

%Set up Channel mode
tc = s.Channels();
    tc.BridgeMode = 'Full';
    tc.NominalBridgeResistance = 150;

%Set Scan Duration
s.DurationInSeconds = 3;
% s.DurationInSeconds = 120;

%Acquires a single scan of data
% data = s.inputSingleScan

[data,timestamps,triggerTime] = startForeground(s);
%returns the data acquired, timestamps relative to the
% time the operation is triggered, and a trigger time
% indicating the absolute time the operation was triggered.

A = [timestamps'; data'];
fileID = fopen('voltreading.txt','w');
fprintf(fileID,'%6s %12s\r\n','time','data');
fprintf(fileID,'%6.2f %12.4f\r\n',A);
fclose(fileID);
% writetable(A,'voltreading.txt');

voltage = max(data)

plot(timestamps,data);
hold on
xlabel('Time(sec)');
ylabel('Voltage');
```

THIS PAGE INTENTIONALLY LEFT BLANK

APPENDIX C. RAW VOLTAGE VS. TIME STRAIN GRAPHS

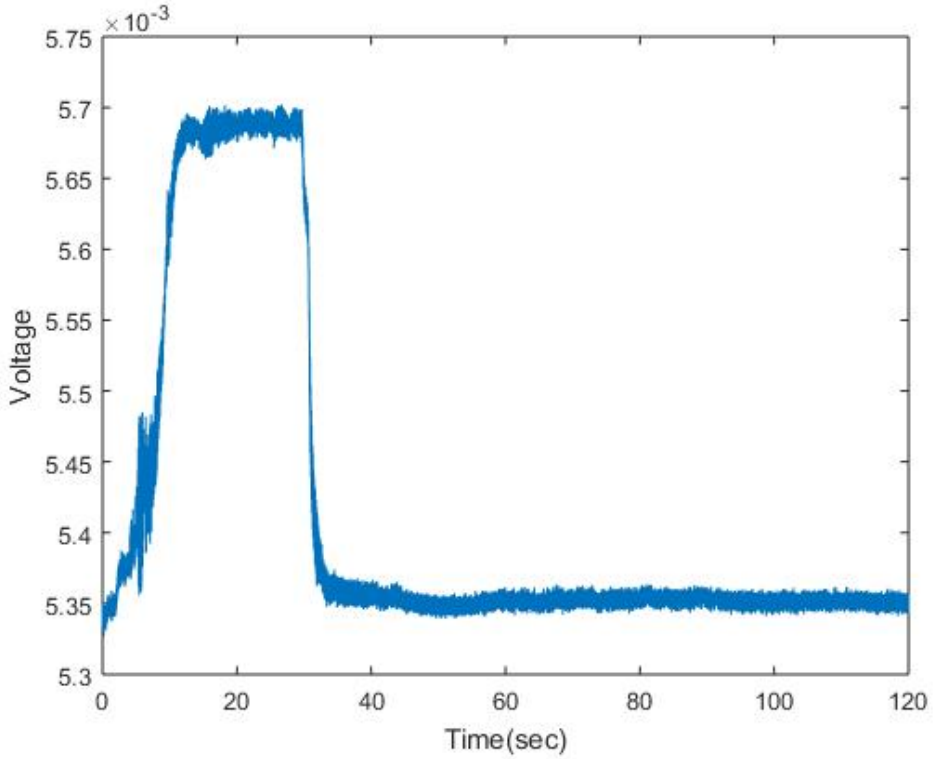

Voltage vs. Time for liquid fuel testing

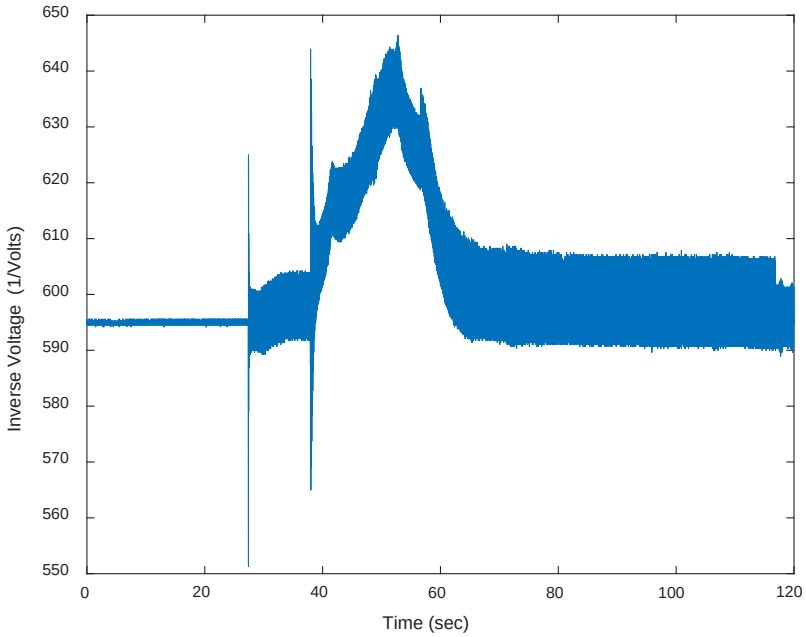

Inverse Voltage vs. Time for hydrogen testing

THIS PAGE INTENTIONALLY LEFT BLANK

APPENDIX D. SPEED EXTRAPOLATION

Thurst (N)	Thrust (lbs)	Speed (rpm)
22.92	5.15	94000.00
26.70	6	98583.92
32.71	7.35	105000.00
43.61	9.8	115000.00
50.20	11.28	123000.00
53.40	12	125764.12
57.85	13	130294.15
62.30	14	134824.18
66.75	15	139354.21

The extrapolation equation was used for 5.15–11.28 lbs of thrust based on the first 4 data points.

The equation was: =TREND(C3:C7,B3:B7,B8:B13,TRUE)

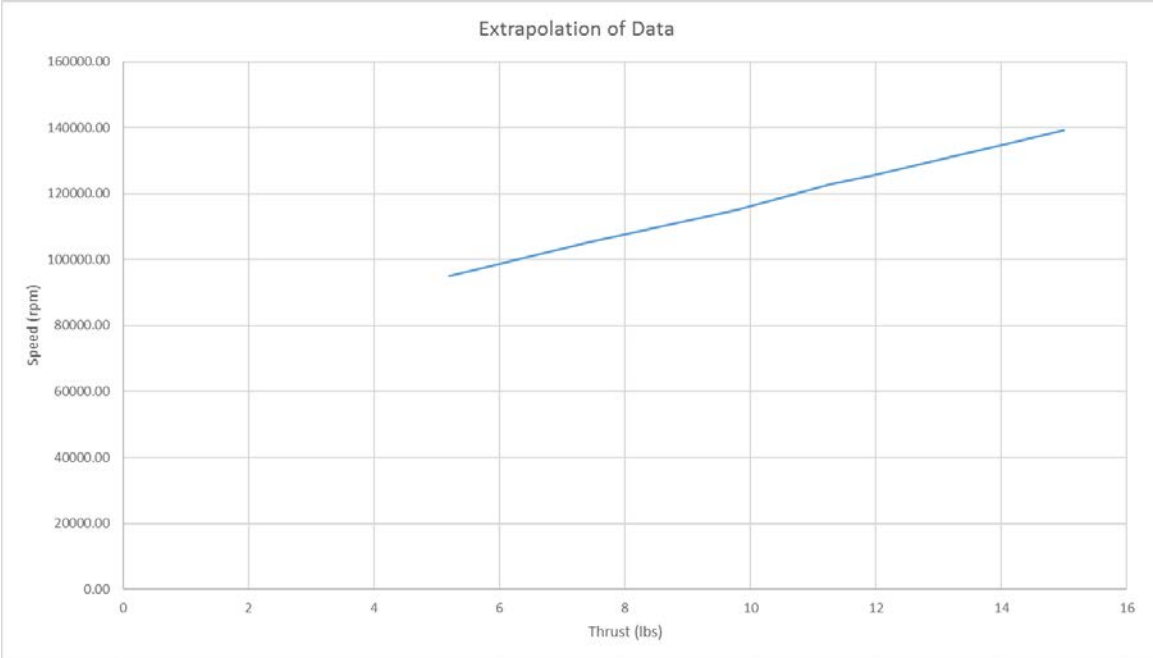

THIS PAGE INTENTIONALLY LEFT BLANK

APPENDIX E. GASTURB CALCULATIONS

Gasturb Calculations in SI units:

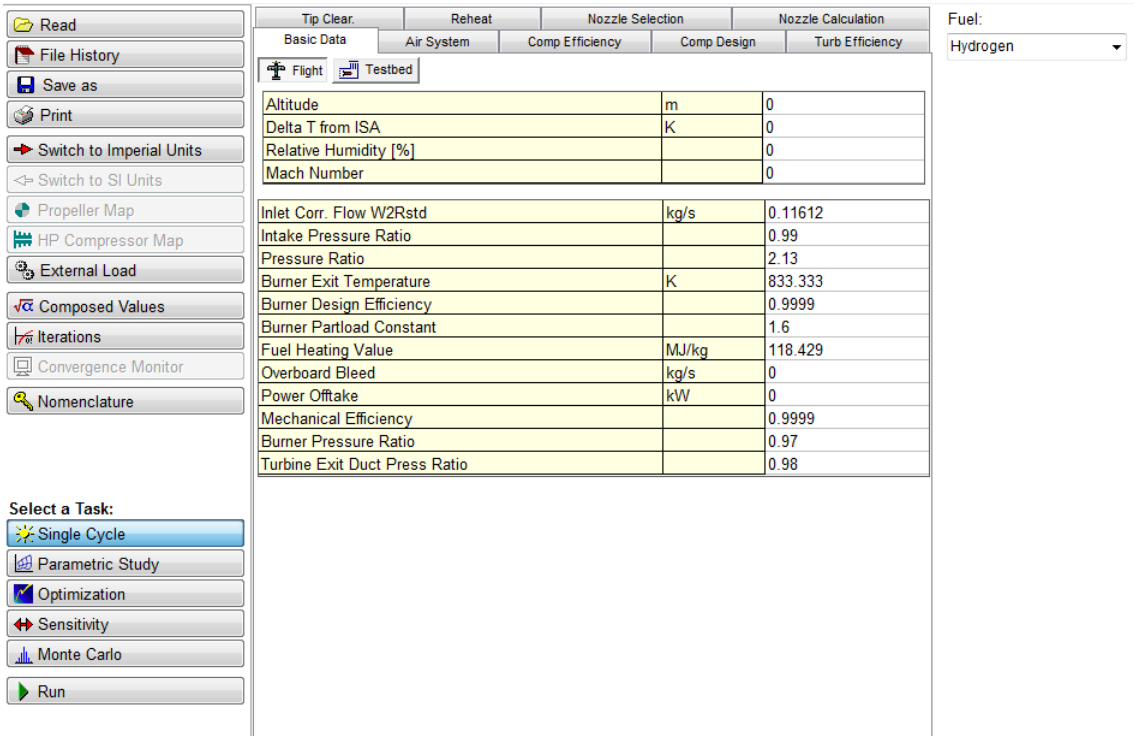

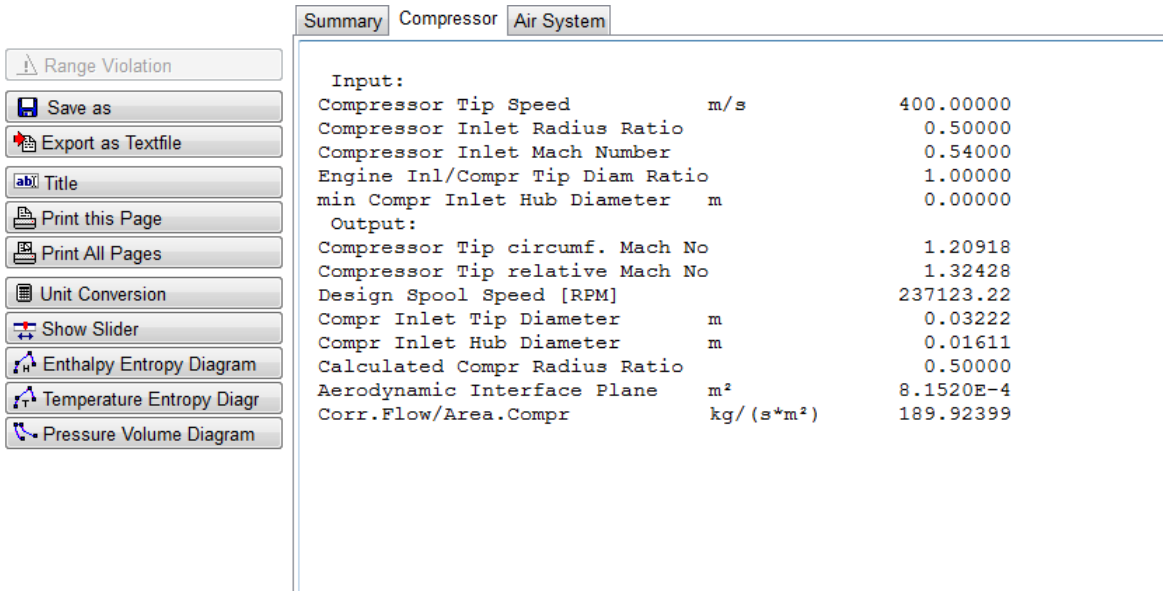

Gasturb Calculations in English units:

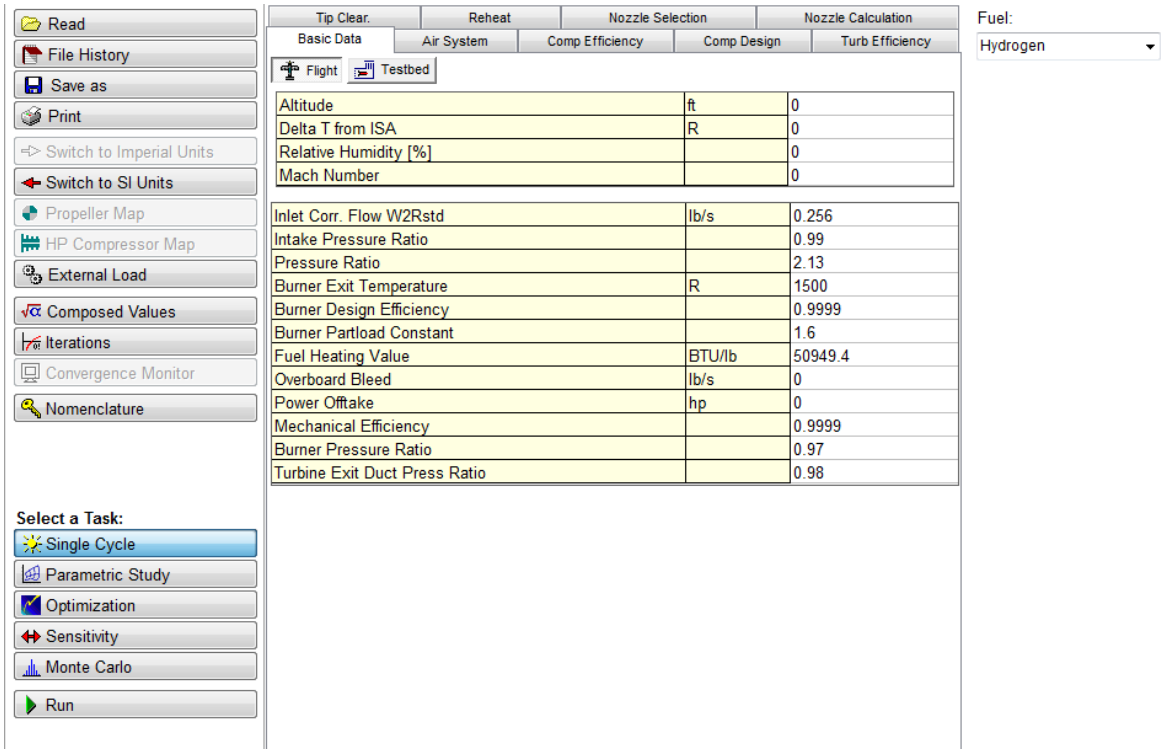

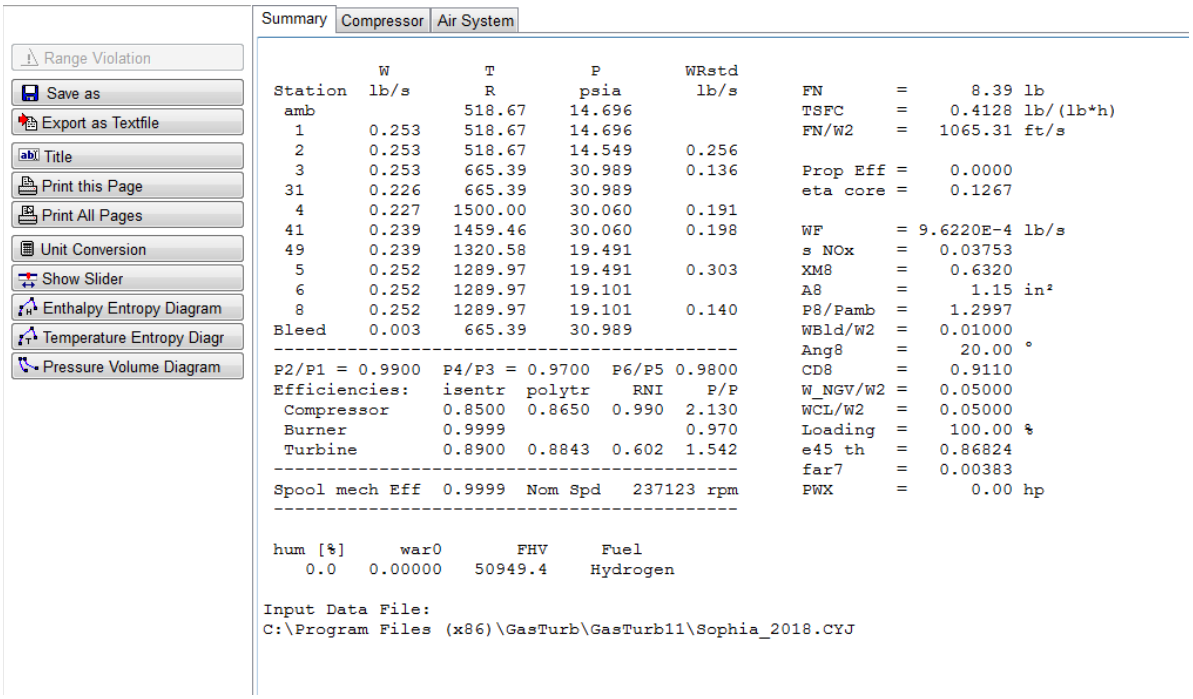
Range Violation
Save as
Export as Textfile
Title
Print this Page
Print All Pages
Unit Conversion
Show Slider
Enthalpy Entropy Diagram
Temperature Entropy Diagr
Pressure Volume Diagram
Summary
Compressor
Air System
W T P WRstd
Station lb/s R psia lb/s
amb 518.67 14.696
1 0.253 518.67 14.696
2 0.253 518.67 14.549 0.256
3 0.253 665.39 30.989 0.136
31 0.226 665.39 30.989
4 0.227 1500.00 30.060 0.191
41 0.239 1459.46 30.060 0.198
49 0.239 1320.58 19.491
5 0.252 1289.97 19.491 0.303
6 0.252 1289.97 19.101
8 0.252 1289.97 19.101 0.140
Bleed 0.003 665.39 30.989
P2/P1 = 0.9900 P4/P3 = 0.9700 P6/P5 0.9800
Efficiencies: isentr polytr RNI P/P
Compressor 0.8500 0.8650 0.990 2.130
Burner 0.9999 0.970
Turbine 0.8900 0.8843 0.602 1.542
Spool mech Eff 0.9999 Nom Spd 237123 rpm
hum [%] war0 FHV Fuel
0.0 0.00000 50949.4 Hydrogen
Input Data File:
C:\Program Files (x86)\GasTurb\GasTurb11\Sophia_2018.CYJ
FN = 8.39 lb
TSFC = 0.4128 lb/(lb*h)
FN/W2 = 1065.31 ft/s
Prop Eff = 0.0000
eta core = 0.1267
WF = 9.6220E-4 lb/s
s NOx = 0.03753
XM8 = 0.6320
A8 = 1.15 in²
P8/Pamb = 1.2997
WBld/W2 = 0.01000
Ang8 = 20.00 °
CD8 = 0.9110
W_NGV/W2 = 0.05000
WCL/W2 = 0.05000
Loading = 100.00 %
e45 th = 0.86824
far7 = 0.00383
PWX = 0.00 hp

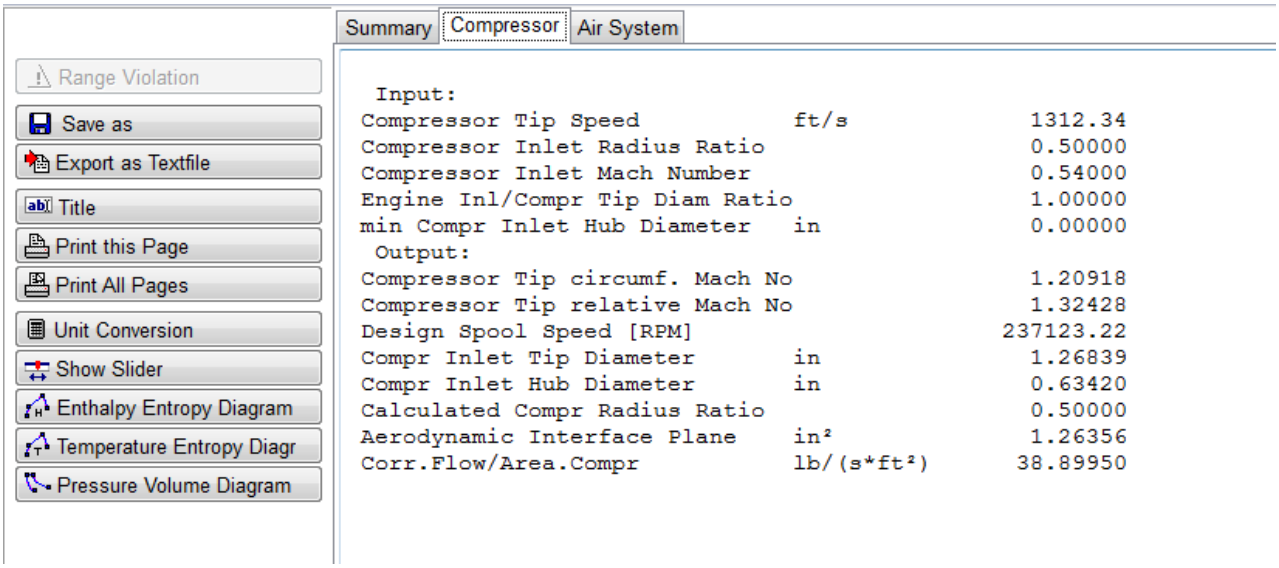
Range Violation
Save as
Export as Textfile
Title
Print this Page
Print All Pages
Unit Conversion
Show Slider
Enthalpy Entropy Diagram
Temperature Entropy Diagr
Pressure Volume Diagram
Summary
Compressor
Air System
Input:
Compressor Tip Speed ft/s 1312.34
Compressor Inlet Radius Ratio 0.50000
Compressor Inlet Mach Number 0.54000
Engine Inl/Compr Tip Diam Ratio 1.00000
min Compr Inlet Hub Diameter in 0.00000
Output:
Compressor Tip circumf. Mach No 1.20918
Compressor Tip relative Mach No 1.32428
Design Spool Speed [RPM] 237123.22
Compr Inlet Tip Diameter in 1.26839
Compr Inlet Hub Diameter in 0.63420
Calculated Compr Radius Ratio 0.50000
Aerodynamic Interface Plane in² 1.26356
Corr.Flow/Area.Compr lb/(s*ft²) 38.89950

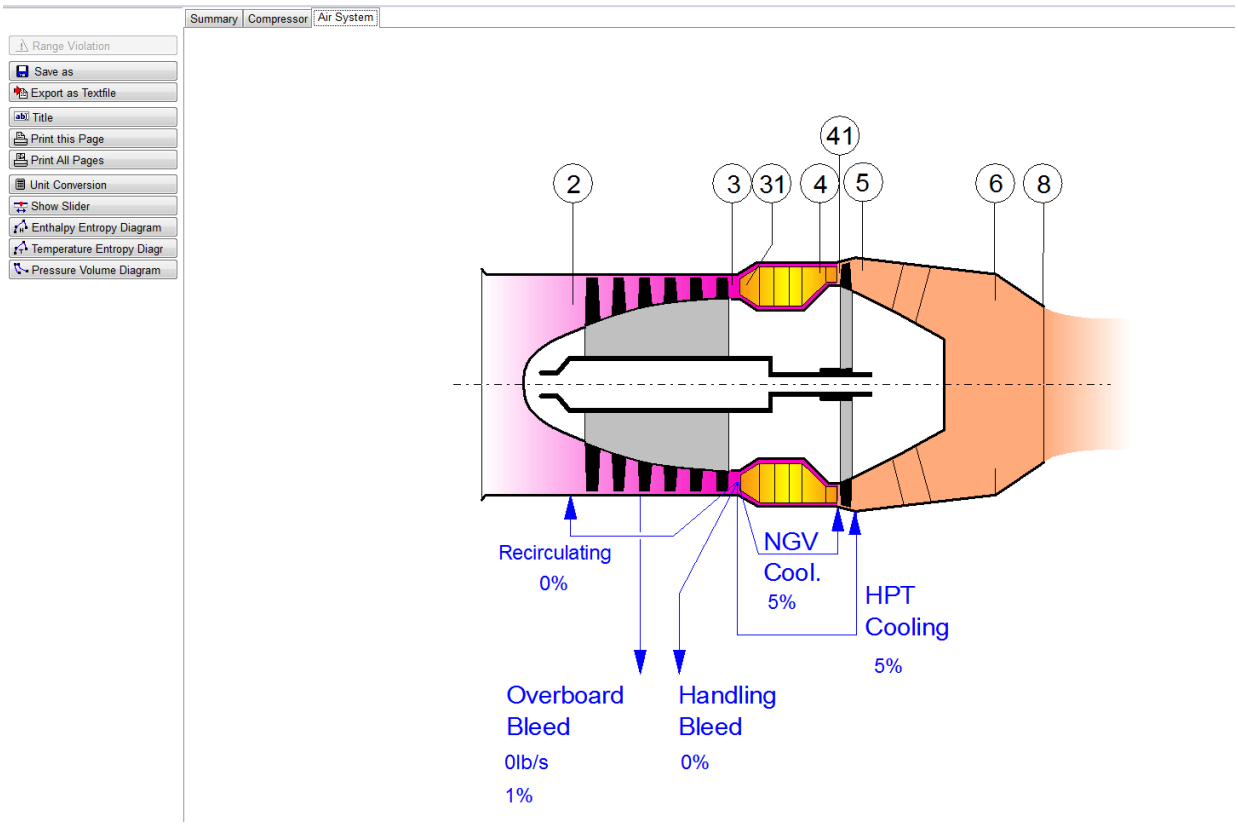
Summary
Compressor
Air System
Range Violation
Save as
Export as Textfile
Title
Print this Page
Print All Pages
Unit Conversion
Show Slider
Enthalpy Entropy Diagram
Temperature Entropy Diagr
Pressure Volume Diagram
41
2
3
31
4
5
6
8
Recirculating
0%
NGV
Cool.
5%
HPT
Cooling
5%
Overboard
Bleed
0lb/s
1%
Handling
Bleed
0%

APPENDIX F. HYDROGEN STANDARD OPERATING PROCEDURE

This procedure was adapted from the Sophia J450 Turbine Engine Instruction Manual and Owners Guide [14].

1. Connect oil pump wiring to remote 12 Volt power supply box prior to engine operation. Fill the oil tank with standard turbine oil. Connect the power supply box to a remote relay to be controlled remotely.
2. Connect the hydrogen supply wiring to the engine fuel injector. Conduct a leak test to ensure the hydrogen piping is tight and secure. Connect hydrogen supply ball valve to a remote relay.
3. Connect the air tubing to the engine. Check for leaks in the air supply connection; any leakage or a poor connection may not allow satisfactory rotation.
4. Ensure the spark plug is operating properly by testing and verifying that an adequate spark is produced. Connect spark leads to engine.
5. For the oil pump: Adjust the voltage of the power supply until the oil pump is running consistently. Ensure oil has reached the engine for at least 2–4 seconds before the engine is started to prime the engine. Once the engine is properly primed, turn off the power supply so that the voltage stays set to the proper reading. When the power supply is plugged into the remote relay, ensure the box is turned on so that when the oil pump is activated, it will turn on accurately.
6. The following items should be created within a remote sequence and operated at a safe distance from the engine:
    a. Start air flow through the engine at 10.54 kg/cm^2 (150 psi).
    b. Switch the spark igniter to on and spark will occur inside the engine.
    c. Start hydrogen flow into the engine at designated pressure. Hydrogen pressure should start low (approximately 14.1 kg/cm^2 (200 psi)) and incrementally increased throughout the run.

i. Be sure to note the pressure limit of the tubing used into the engine, as a hard line may be needed for higher pressures.

7. The turbine rotation sound level should be very high. If the sound level is not high or if you hear an abnormal sound, stop the engine immediately. Ensure to incorporate an emergency abort in the remote operating sequence.
8. After combustion starts, continue the air supply and spark until the compressor pressure is about .3 kg/cm^2 (4 psi) on the compressor pressure gauge, then stop the ignitor and start air.
9. If the engine does not start within 10 seconds, abort engine operation and cool down the engine with 7 kg/cm^2 (100 psi) cooling air. Then drain excess fuel from inside of engine by holding engine vertical. Fuel can also be flushed from the system by keeping oil on and running the cooling air through the engine.
10. Confirm the flow lubrication oil are normal while operating. For maximum output, increase the hydrogen supply pressure until compressor pressure reaches 1.3 kg/cm2 (18 psi). The rpm at this state is about 123,000 rpm, and the thrust is over 48.9 N (11 lbs). To ensure the engine does not over speed, a conditional statement in the remote sequence to initiate cool down at this limit might be implemented.
    a. Never exceed 1.3 kg/cm2 (18.3 psi) compressor ratio. This is regulated by the supply of hydrogen to the engine. Decrease the hydrogen pressure to decrease the compressor ratio.
11. If at any time, the lubrication oil is completely consumed, cut power to the hydrogen supply immediately.
12. If a long flame blows out the tail pipe, breakage in the engine, or leakage of the piping, stop the engine immediately by cutting power to the fuel pump, and extinguish is necessary.
13. The engine remains hot for about 1 hour after stopping. Take care when handling.
14. After running, disconnect power to the hydrogen supply and oil pump.

APPENDIX G. GASTURB THRUST PREDICTIONS COMPARING LIQUID FUEL AND HYDROGEN

Data in SI units:

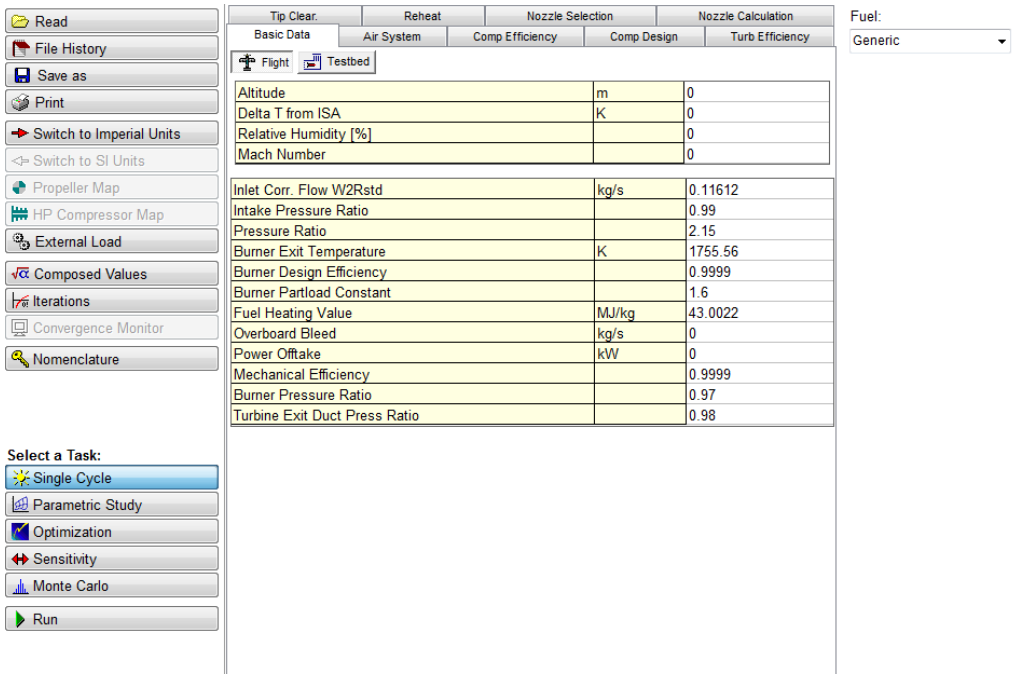

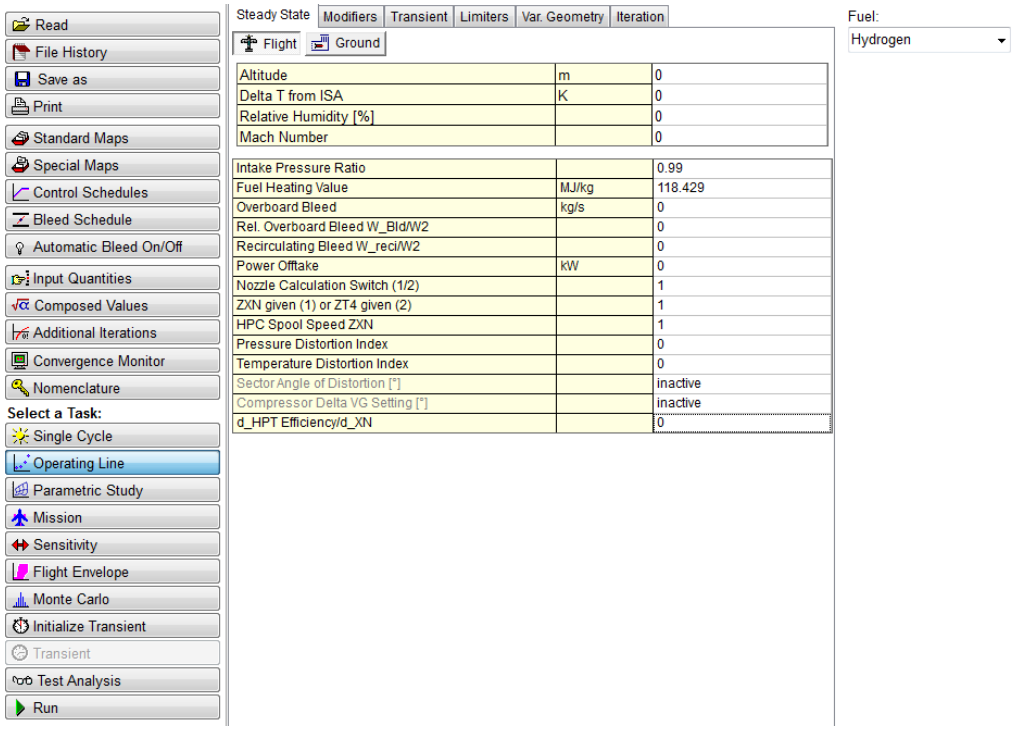

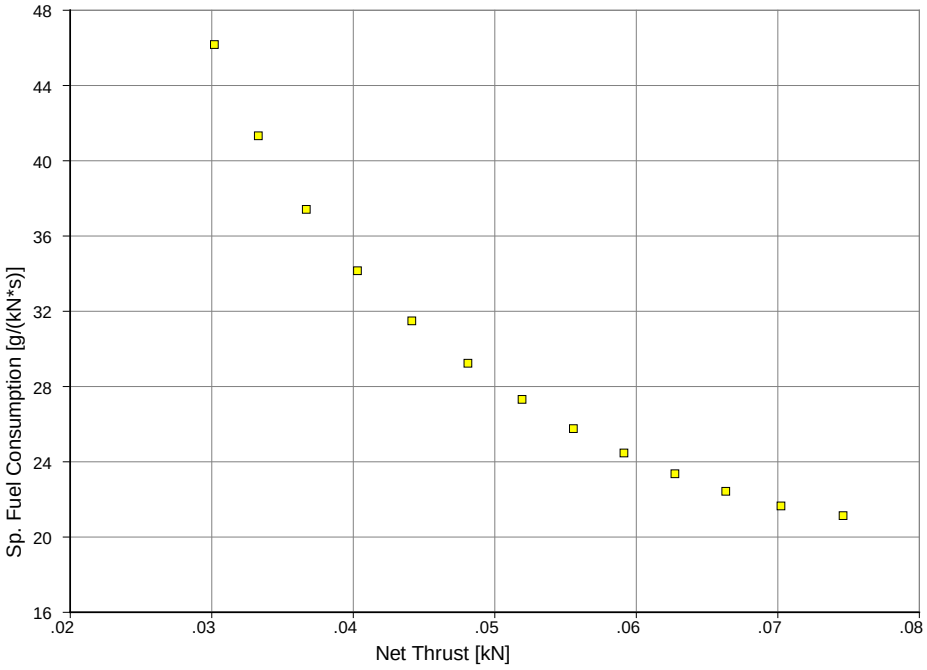

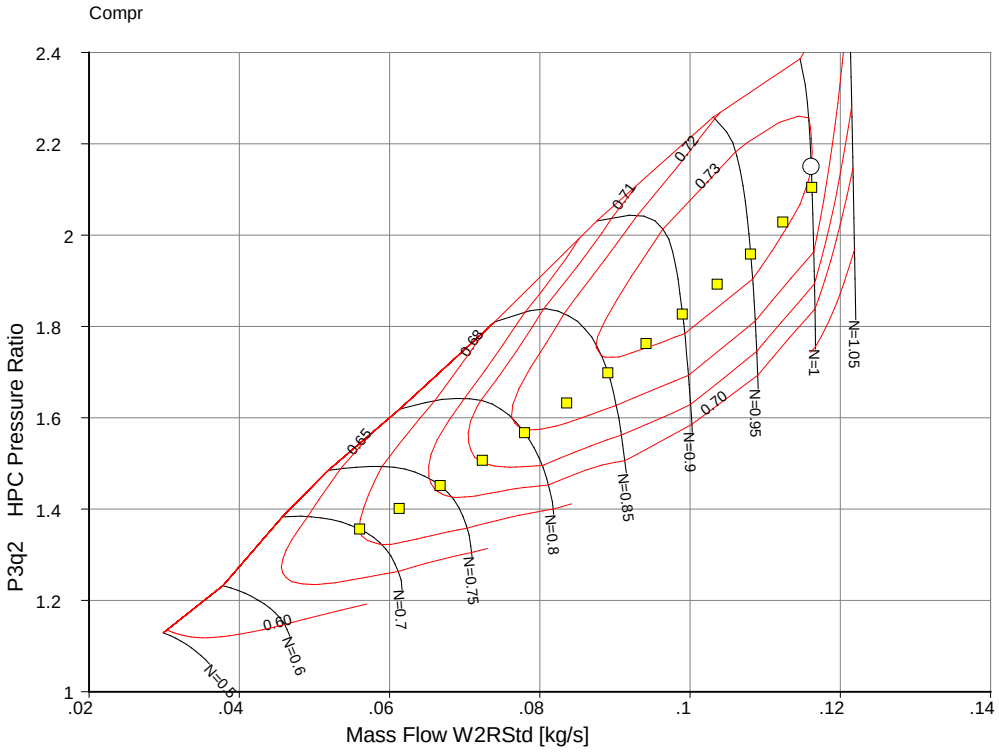

Data in English units:

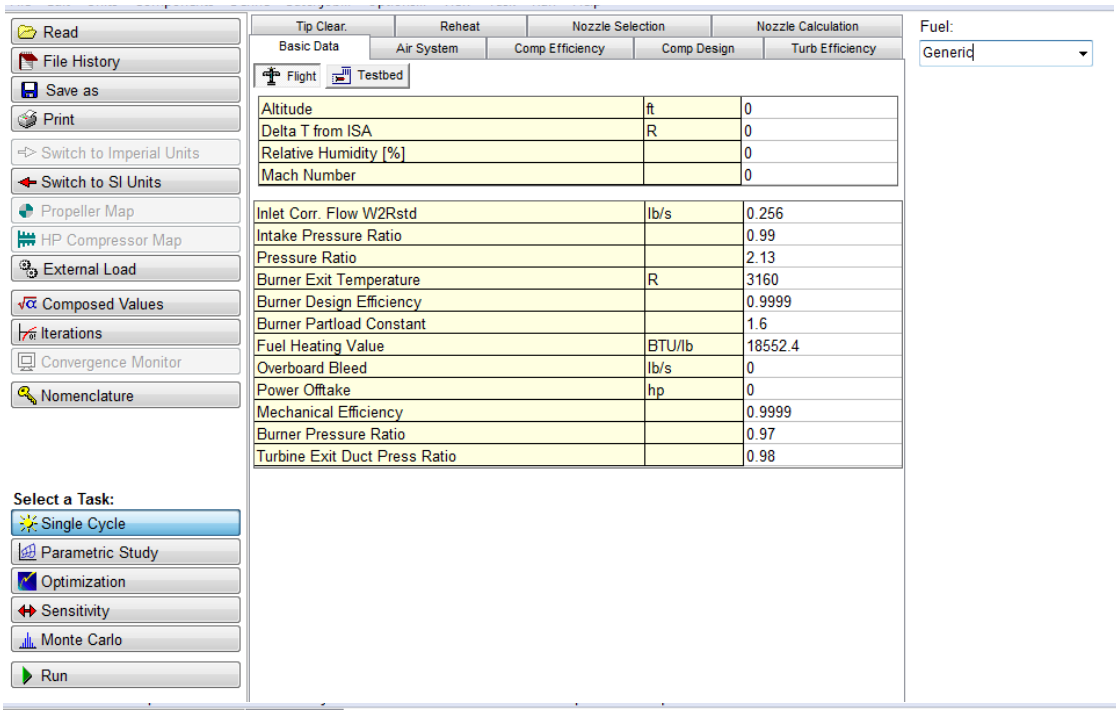
Read
File History
Save as
Print
Switch to Imperial Units
Switch to SI Units
Propeller Map
HP Compressor Map
External Load
Composed Values
Iterations
Convergence Monitor
Nomenclature
Select a Task:
Single Cycle
Parametric Study
Optimization
Sensitivity
Monte Carlo
Run
Tip Clear.
Reheat
Nozzle Selection
Nozzle Calculation
Basic Data
Air System
Comp Efficiency
Comp Design
Turb Efficiency
Flight
Testbed
Altitude ft 0
Delta T from ISA R 0
Relative Humidity [%] 0
Mach Number 0
Inlet Corr. Flow W2Rstd lb/s 0.256
Intake Pressure Ratio 0.99
Pressure Ratio 2.13
Burner Exit Temperature R 3160
Burner Design Efficiency 0.9999
Burner Partload Constant 1.6
Fuel Heating Value BTU/lb 18552.4
Overboard Bleed lb/s 0
Power Offtake hp 0
Mechanical Efficiency 0.9999
Burner Pressure Ratio 0.97
Turbine Exit Duct Press Ratio 0.98
Fuel:
Generic

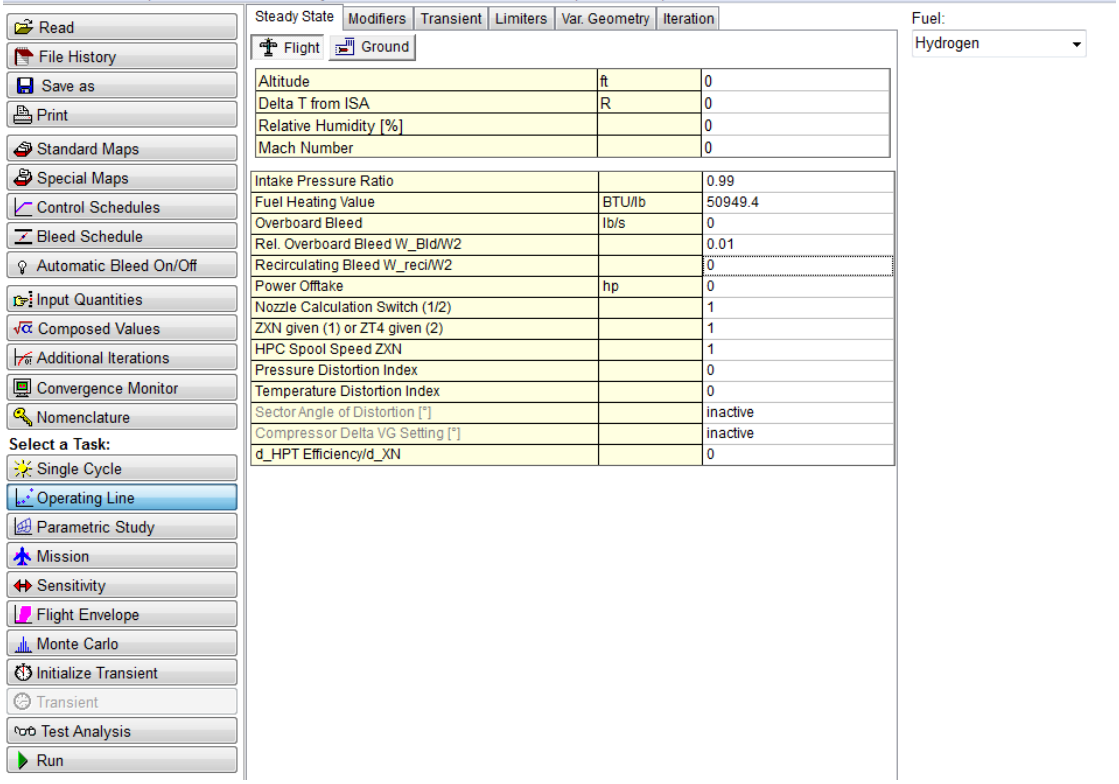
Read
File History
Save as
Print
Standard Maps
Special Maps
Control Schedules
Bleed Schedule
Automatic Bleed On/Off
Input Quantities
Composed Values
Additional Iterations
Convergence Monitor
Nomenclature
Select a Task:
Single Cycle
Operating Line
Parametric Study
Mission
Sensitivity
Flight Envelope
Monte Carlo
Initialize Transient
Transient
Test Analysis
Run
Steady State
Modifiers
Transient
Limiters
Var. Geometry
Iteration
Flight
Ground
Altitude ft 0
Delta T from ISA R 0
Relative Humidity [%] 0
Mach Number 0
Intake Pressure Ratio 0.99
Fuel Heating Value BTU/lb 50949.4
Overboard Bleed lb/s 0
Rel. Overboard Bleed W_Bld/W2 0.01
Recirculating Bleed W_reci/W2 0
Power Offtake hp 0
Nozzle Calculation Switch (1/2) 1
ZXN given (1) or ZT4 given (2) 1
HPC Spool Speed ZXN 1
Pressure Distortion Index 0
Temperature Distortion Index 0
Sector Angle of Distortion [°] inactive
Compressor Delta VG Setting [°] inactive
d_HPT Efficiency/d_XN 0
Fuel:
Hydrogen

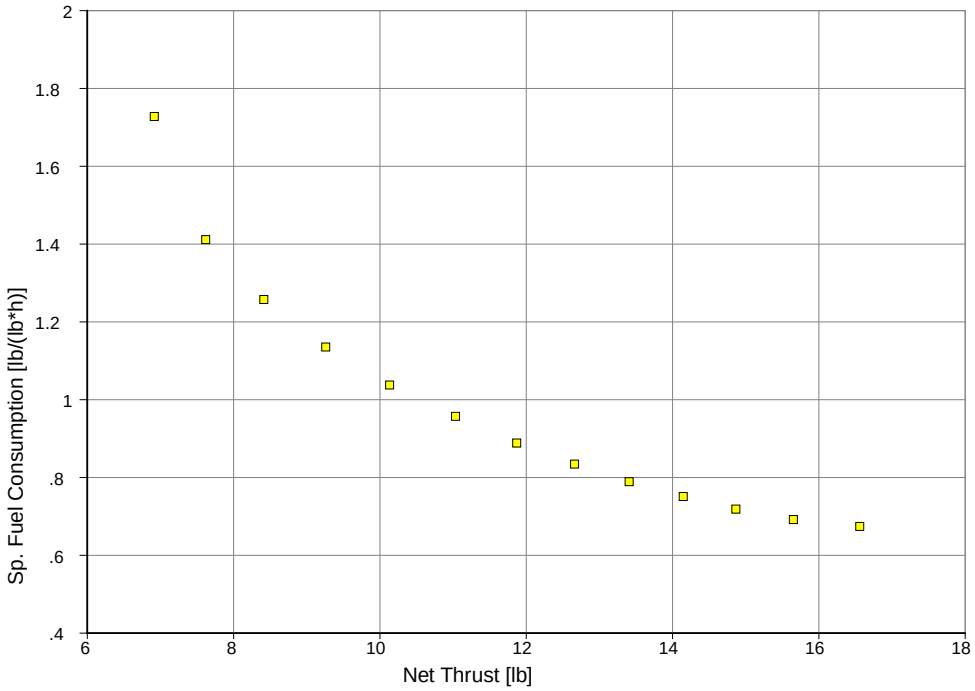
Sp. Fuel Consumption [lb/(lb*h)]
2
1.8
1.6
1.4
1.2
1
.8
.6
.4
6
8
10
12
14
16
18
Net Thrust [lb]

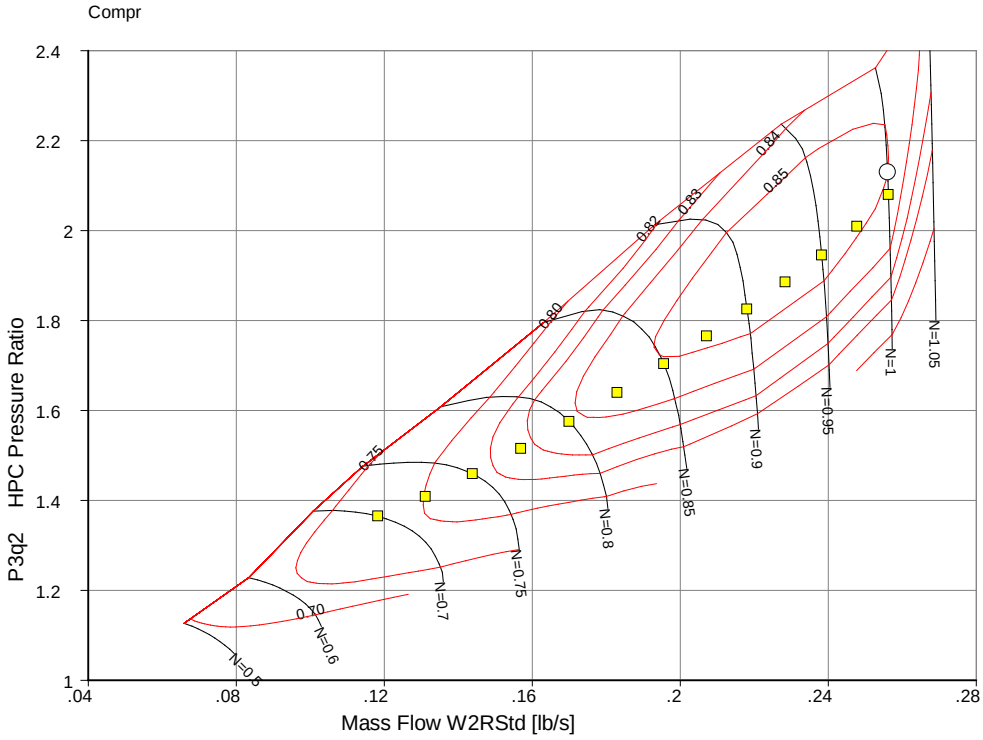
Compr
P3q2 HPC Pressure Ratio
2.4
2.2
2
1.8
1.6
1.4
1.2
1
.04
.08
.12
.16
.2
.24
.28
Mass Flow W2RStd [lb/s]
0.84
0.85
0.83
0.82
0.80
0.75
0.70
N=0.5
N=0.6
N=0.7
N=0.75
N=0.8
N=0.85
N=0.9
N=0.95
N=1
N=1.05

APPENDIX H. GASTURB HYDROGEN ANALYSIS

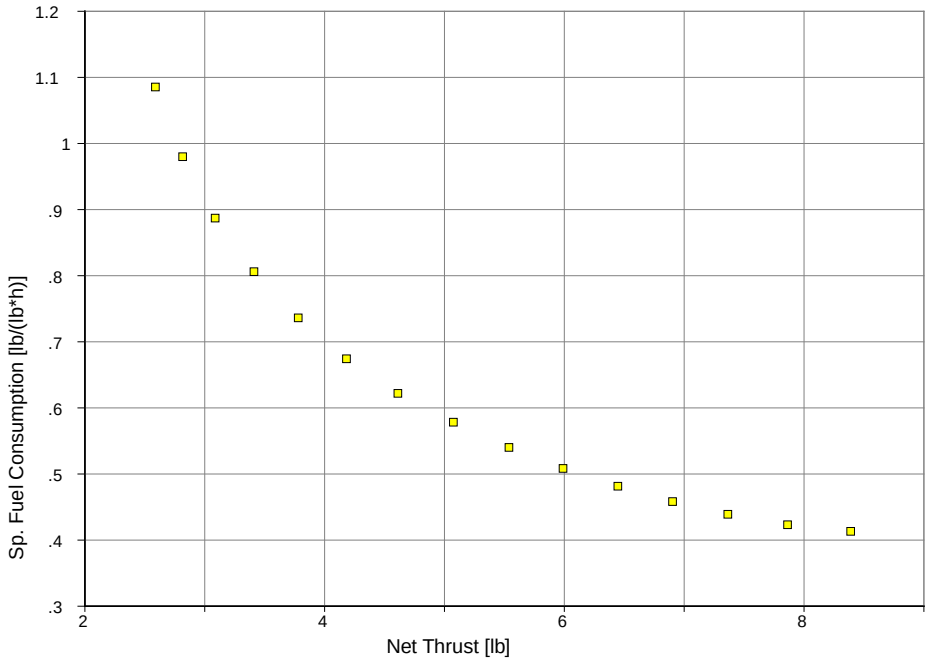

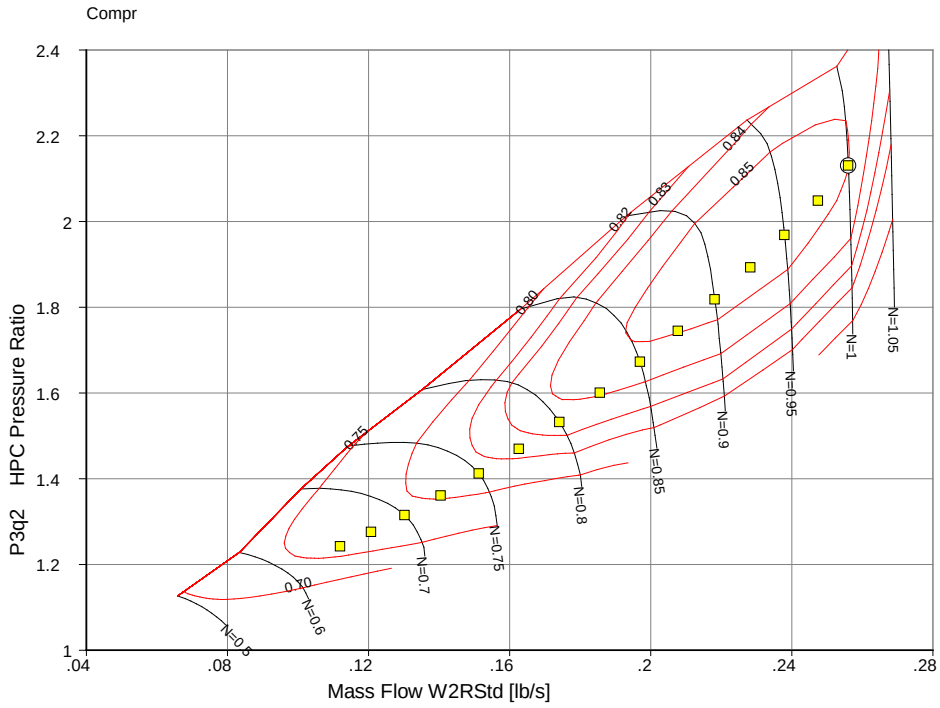

THIS PAGE INTENTIONALLY LEFT BLANK

LIST OF REFERENCES

[1] Deputy Assistant Secretary of the Navy Energy Office, "Department of the Navy Strategy for Renewable Energy," Washington, DC, USA, 2012. [Online] Available: http://www.secnav.navy.mil/eie/Documents/DoNStrategyforRenewableEnergy.pdf

[2] Office of the Assistant Secretary of Defense for Energy, Installations, and Environment, "Department of Defense Annual Energy Management and Resilience (AEMR) Report Fiscal Year 2016," Washington, DC, USA, 2017. [Online] Available: https://www.acq.osd.mil/eie/Downloads/IE/FY%202016%20AEMR.pdf

[3] Conserve Energy Future, "What is Hydrogen Energy?," from https://www.conserve-energy-future.com/advantages_disadvantages_hydrogenenergy.php

[4] Airforce Print News, "Hickam testing new deployable hydrogen refueling station," from https://www.af.mil/News/Article-Display/Article/129227/hickam-testing-new-deployable-hydrogen-refueling-station/

[5] Clean Energy Resource Teams, "Fuel Cells and Microturbines," from https://www.cleanenergyresourceteams.org/files/CERTsManualCh11.pdf

[6] K. Bennaceur, B. Clark, F. M. Orr, Jr., T. S. Ramakrishnan, C. Roulet, E. Stout, "Hydrogen: A Future Energy Carrier?," *Oilfield Review*, 2005. [Online] Available: https://pdfs.semanticscholar.org/3a43/1edc56da50328db89dd9bd8aaa447d7b0d07.pdf.

[7] V. Knop, A. Benkenida, S. Jay, and C. Oliver. "Modelling of combustion and nitrogen oxide formation in hydrogen-fuelled internal combustion engines within a 3D CFD code." *International Journal of Hydrogen Energy* Vol. 33 No. 19 (2008): pp. 5083–5097. https://www.sciencedirect.com/science/article/pii/S0360319908007246.

[8] Enel S.p.A., 2010, "Enel: At Fusina (Venice), Inauguration of First Industrial-Scale Hydrogen Plant in the World," from https://www.enel.com/media/press/d/2010/07/enel-at-fusina-venice-inauguration-of-first-industrial-scale-hydrogen-plant-in-the-world .

[9] Engineering Tech, 2007, " Hydrogen turbines generate clean electricity," from https://www.zdnet.com/article/hydrogen-turbines-generate-clean-electricity/

[10] A. Aviles, “Renewable production of water, hydrogen, and power from ambient moisture,” M.S. thesis, Mech Egr. Dept., Naval Postgraduate School, Monterey, CA, USA, 2016. [Online]. Available: https://calhoun.nps.edu/handle/10945/51584

[11] S. F. Yu, “Analysis of an improved solar-powered hydrogen generation system for sustained renewable energy production,” M.S. thesis, Mech. Egr. Dept., Naval Postgraduate School, Monterey, CA, USA, 2017. [Online] Available: https://calhoun.nps.edu/handle/10945/56854.

[12] S. M. Birkemeier, “Industrial automation of solar-powered hydrogen generation plant,” M.S. thesis, Mech. Egr. Dept., Naval Postgraduate School, Monterey, CA, USA 2017. [Online] Available: https://calhoun.nps.edu/handle/10945/59700 .

[13] E. A. Fosson, “Design and analysis of a hydrogen compression and storage station,” M.S. thesis, Mech. Egr. Dept., Naval Postgraduate School, Monterey, CA, USA 2017. [Online] Available: https://calhoun.nps.edu/handle/10945/56919.

[14] Sophia J450 Turbine Engine Instruction Manual and Owner’s Guide, p. 3.

[15] Capstone MicroTurbine Model C30 User’s Manual, pp. 14–18.

[16] U.S. OSHA, “Material Safety Data Sheet Product: Coleman Fuel,” from http://www.farnell.com/datasheets/1700915.pdf

[17] H. Garcia, “Testing and development of a shrouded gas turbine engine in a freejet facility,” M.S. thesis, Mech. Egr. Dept., Naval Postgraduate School, Monterey, CA, USA 2000. [Online] Available: https://calhoun.nps.edu/handle/10945/7809.

[18] C. Borgnakke and R. E. Sonntag, *Fundamentals of Thermodynamics*, 8th ed., Danvers, MA: John Wiley & Sons, Inc., 2013.

[19] Engineering Toolbox, 2003. “Flame Temperature Gases.” from https://www.engineeringtoolbox.com/flame-temperature-gases-d_442.html

[20] H. Chu, “Flame Temperature,” Department of Environmental Engineering, National Cheng Kung University, [Online] Available: http://myweb.ncku.edu.tw/~chuhsin/ppt/combustion%20principles%20and%20control/04-Flame%20Temperature.ppt

INITIAL DISTRIBUTION LIST

1. Defense Technical Information Center
   Ft. Belvoir, Virginia

2. Dudley Knox Library
   Naval Postgraduate School
   Monterey, California